NATIONAL AERONAUTICS AND SPACE ADMINISTRATION

Technical Report 32-1321

Mariner Venus 67 Solar Panel

J. V. Goldsmith
W. Hasbach
R. Yasui

JET PROPULSION LABORATORY
CALIFORNIA INSTITUTE OF TECHNOLOGY
PASADENA, CALIFORNIA

April 15, 1970

Technical Report 32-1321

Mariner Venus 67 Solar Panel

J. V. Goldsmith

W. Hasbach

R. Yasui

Preface

The work described in this report was performed by the Guidance and Control Division of the Jet Propulsion Laboratory.

Contents

Tables

Contents (contd)

Figures

Contents (contd)

Figures (contd)

Abstract

This document describes the design, manufacture, assembly, testing, and performance of the solar array that was used for the *Mariner* Venus 67 mission. Also included are remarks on the adequacy of the solar array design and recommendations for the design of solar panels for future missions of the *Mariner* Venus 67 type.

Mariner Venus 67 Solar Panel

I. Introduction

The *Mariner* Venus 67 solar array was designed to meet the raw electrical power requirements and environmental extremes that would be experienced during the spacecraft mission to Venus. A basic ground rule associated with this design was that it would employ *Mariner* Mars 1964 technology wherever possible to minimize the impact on development schedule and cost. Functional requirements of the design of the solar arrays were that it provide:

(1) A minimum of 360 W power at a space solar intensity of 135 mW/cm^2 and 58°C.

(2) A voltage output from the array limited to 50 V.

(3) A maximum power voltage of 44 ±2 V.

(4) Panel weight less than 15.7 lb.

II. Design and Manufacture

The *Mariner* Venus 67 spacecraft solar array included four oriented solar panels (Fig. 1), each having 10.9 ft^2 of area available for solar cell mounting. The cell layout on each solar panel consisted of a "folded" string (Fig. 2), which, after deployment, was maintained in a plane perpendicular to the Z-axis of the spacecraft. For improved reliability, each panel was divided into three isolated electrical sections that consisted of two folded strings of 105 cells in series and 14 cells in parallel. The solar cells used in the design are 1 × 2-cm p-on-n (p–n) silicon solar cells interconnected into seven cell submodules with gold-plated Kovar bus bars.

The electrical schematic of a typical electrical section is shown in Fig. 3. Basically, the electrical design was similar to that employed for the *Mariner* Mars 1964 solar panel. Similar materials, submodules, and techniques were incorporated wherever possible. New materials that were
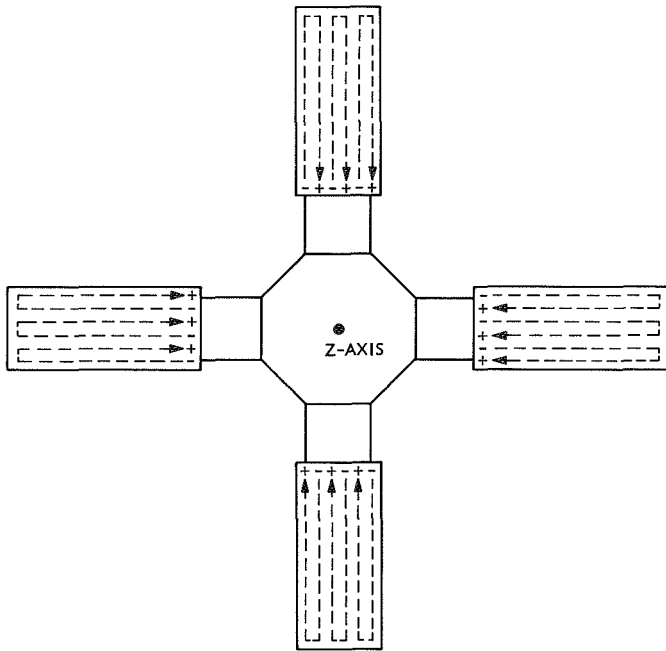
Fig. 1. Solar panel layout in relation to spacecraft

concept minimized the magnetic field generated by the solar cell current; this was achieved through the cancellation of fields as a result of so positioning adjacent current paths that the current flowed in opposite directions. In addition, the voltage strings all terminated at the inboard edge of the panel, thereby greatly simplifying the cabling required. The longitudinal orientation of the strings also reduced the possibility of the loss of a complete panel (three voltage strings) as a result of shroud damage during the shroud-separation event. The output of each electrical section of the array was shunt-regulated by a string of six zener diodes to limit the voltage output to less than 50 V. To provide good heat sinking and radiation to space, the zeners were mounted on the supporting spars of the array structure.

selected for use in the *Mariner* Venus 67 Project after analysis and testing were the following:

Item	*Mariner* Venus 67 configuration material
Dielectric insulation	Epon 956/108 Volan A cloth coating rather than SMP-62/63
Splice insulation	Kynar sleeving rather than Thermofit sleeving
Circuit insulation	Printed circuit boards conformal-coated with 1C2 rather than laminated circuit boards

Physical and performance characteristics of the *Mariner* Venus 67 solar array are shown in Table 1. A comparison of solar panel weights by component for the *Mariner* Mars 1964 and *Mariner* Venus 67 configurations is shown in Table 2.

The cell layout and cable routing were designed to minimize the magnetic fields caused by solar panel current flow and materials. The use of the folded electrical section

Fig. 2. Folded solar cell layout

27 SUBMODULES

26 SUBMODULES

26 SUBMODULES

26 SUBMODULES

7-CELL SUBMODULE
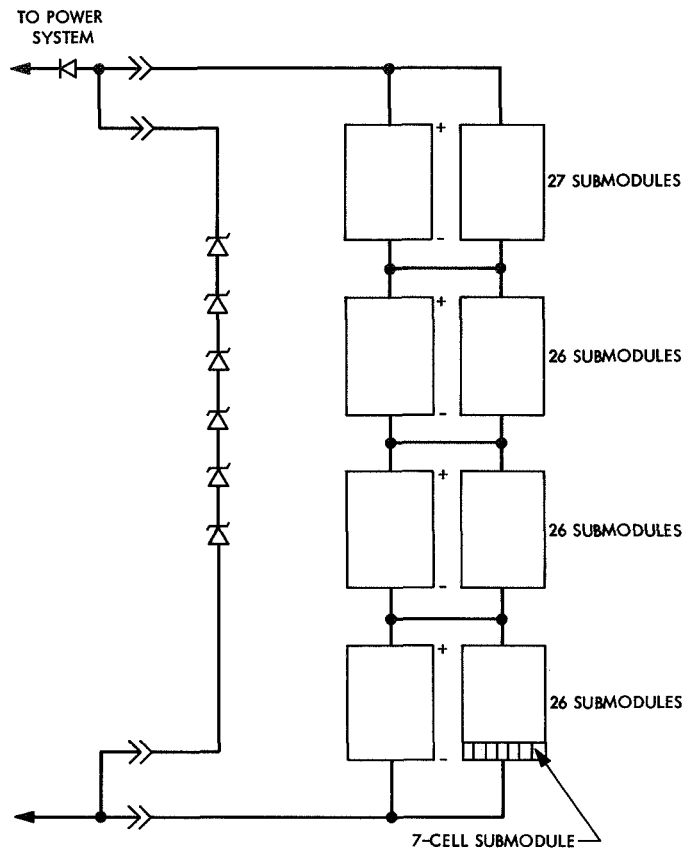
Fig. 3. Schematic drawing of typical electrical section

Table 1. Physical and performance characteristics of the *Mariner* Venus 67 solar array

Item	Characteristic
Solar panel area	10.9 ft² (35.5 × 44.40 in.)
Total solar panel area per spacecraft	43.6 ft² (4 panels)
Number of cells per panel (including packing factor)	4410 (404 cells/ft² × 10.9 ft²)
Number of cells per spacecraft	16,640 (4410 × 4)
Submodule size	2 × 7 cm (1 series × 7 parallel, *Mariner* Mars 1964 type)
Number of submodules per panel	630
Number of submodules per spacecraft	2520 (630 × 4)
Number of sections per panel	3
Panel matrix	105 cells in series, 42 cells in parallel (3 sections)

Table 1 (contd)

Item	Characteristic
Spacecraft matrix	105 cells in series, 168 cells in parallel (12 sections)
Estimated power in near-earth space	100 W/panel
Spacecraft raw power in near-earth space	400 W

Table 2. Comparison of solar panel weights by component, *Mariner* Mars 1964 and *Mariner* Venus 67 configurations

Component[a]	Weight, lb	
	Mariner Mars 1964 configuration	*Mariner* Venus 67 configuration
Structure	10.20	9.0
Dielectric coating	0.50	0.5
Submodules (1008)[b] Cells Filters Bus bars	5.60	3.5
Zener diodes (24)[c] and mounting hardware	1.04	0.78
Harness and connector	0.51	0.35
Adhesives RTV-40 RTV-60 Epon 910 Eccocoat 200	0.40	0.3
Resistors (4)	0.004	0.004
Temperature transducers	0.001	0.001
I_{sc}–V_{oc} transducer	0.010	0.010
Circuit terminal board	0.200	0.175
Cable clamps (32) and washers	0.250	0.250
Grommets (40) and bushings	0.150	0.150
Screws (36), nuts, and washers	0.230	0.230
Total	19.1	15.25

[a]Numbers in parentheses indicate numbers of components in *Mariner* Mars 1964 configuration.
[b]Total of 630 in *Mariner* Venus 67 configuration.
[c]Total of 18 in *Mariner* Venus 67 configuration.

Additional features of the *Mariner* Venus 67 solar array included four transducers to aid in monitoring the array operating temperature and a short-circuit current and open-circuit voltage (I_{sc}–V_{oc}) transducer (Figs. 4–7).

A. Solar Panel Substrate

The *Mariner* Venus 67 solar panel substrate (see Fig. 4) was fabricated for JPL by the Aerospace Division of Ryan Aeronautical Co. of San Diego, Calif. The substrate was an all-aluminum bonded structure and was composed of a 4-mil skin reinforced with lateral 3-mil corrugations. This substrate composite matrix was supported over its entire length by two parallel box beam spars with 10-mil webs and a 20-mil cap. The skin and spars were bonded together with Shell Epon 913 adhesive.

The vertical elements of the corrugation and the spars were pierced with flanged holes to minimize weight and to promote heat radiation from the backside of the skin. The entire back surface of the panel was coated with a high-emissivity-gloss black paint (Laminar X-500, Magna Coatings and Chemical Corp., Los Angeles, Calif.). The cell surface of the substrate skin was covered with 3-mil-thick, epoxy-impregnated fiber glass to provide an electrically insulating layer on which to mount the solar cells. The resulting solar panel substrate weighed approximately 9 lb.

Control of the panel quality and safety during fabrication was strictly maintained by Ryan and JPL inspectors. This structure, which was later loaded with solar cells and zener diodes to approximately the same weight as the substrate itself, could have been damaged seriously by relatively minor accidents and, therefore, required special protection. After fabrication and before final acceptance, the solar array structure assembly was subjected to a thorough final inspection by JPL Quality Assurance to ensure the integrity of dimensional tolerances. Tolerances that were inspected included skin surface flatness, bond fillets, and dielectric strength of the insulating coating. In addition, all panels were subjected to ultrasonic inspection to ensure good adhesion of skin, corrugation, and spars.

B. Zener Diode Shunt Regulator

The flight configuration of the *Mariner* Venus 67 solar array shunt regulator required six Dickson 50 SZ 7.5D zener diodes connected in series for each electrical section of a panel. The diodes were torqued to the underside of the panel box beam spars that provide the heat sink for diode temperature control. The anticipated worst-case
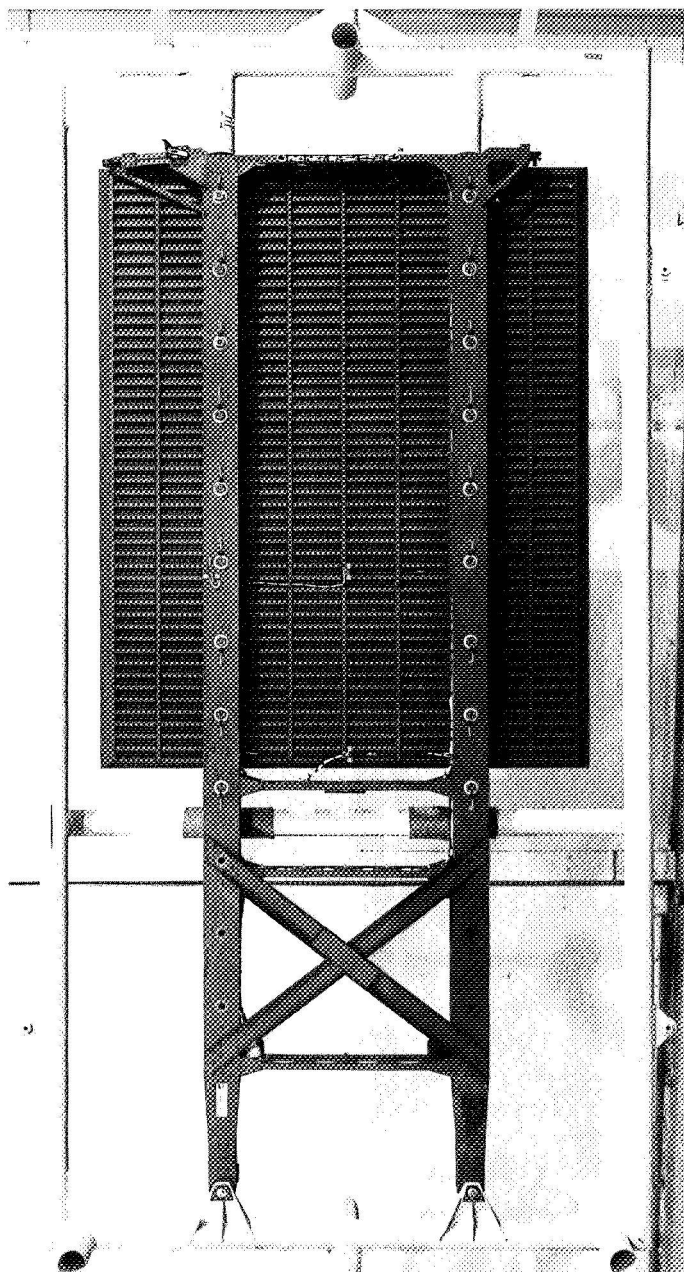
Fig. 4. Solar panel rear surface

power dissipation was 10.5 W per diode. The diodes were electrically insulated from the spars with 6-mil mica washers; after installation, they were coated with Laminar X-500 black paint to improve surface emissivity.

The diodes were procured from Dickson according to JPL specification and had the following nominal characteristics: a zener voltage of 8.25 V ±2% at 1 A and a 90°C stud temperature, and a temperature coefficient of 3.27 ±0.72 mV/°C. Results of testing and analysis
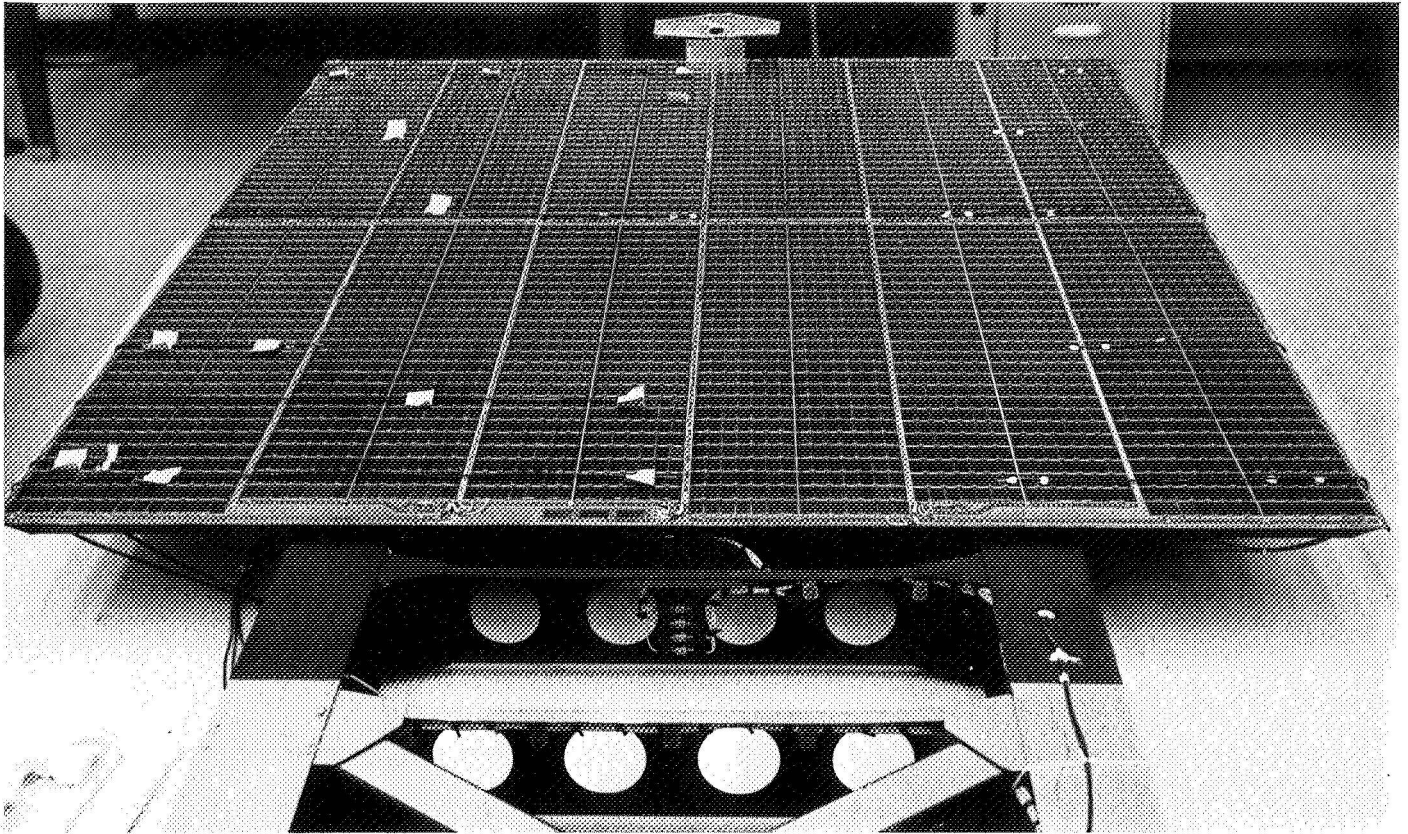
Fig. 5. Solar panel front surface
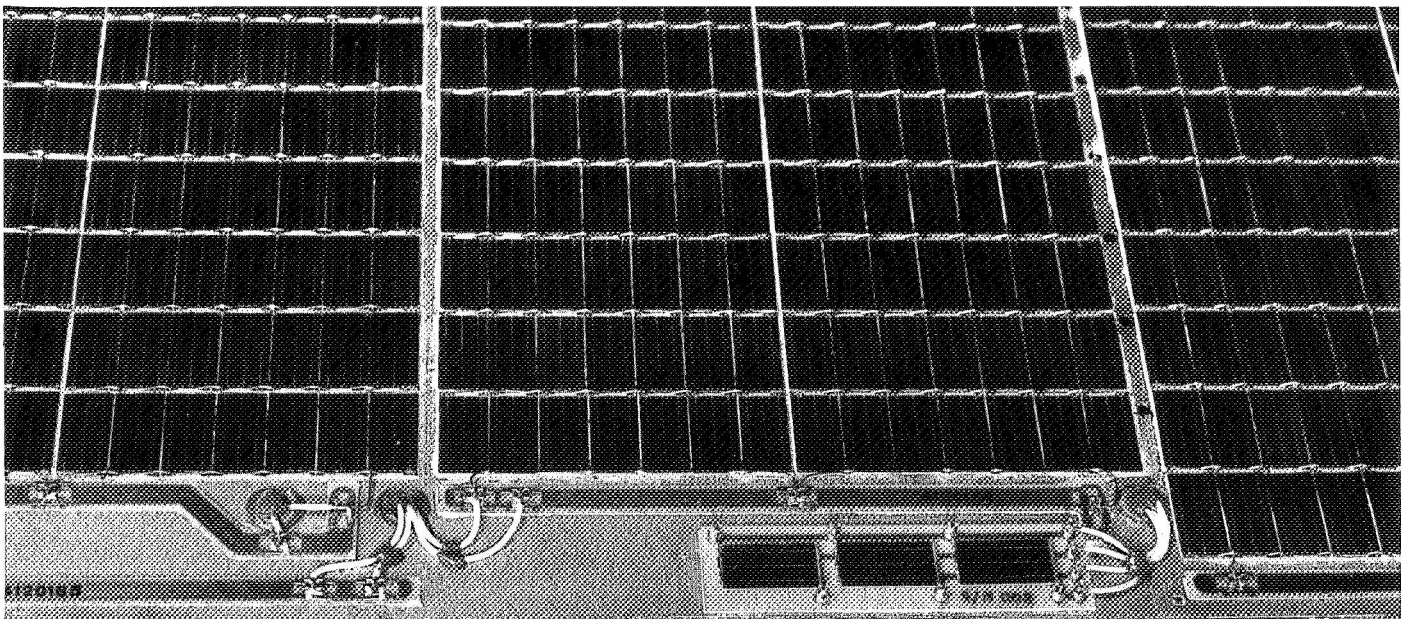
Fig. 6. Close up view of I_{sc}–V_{oc} transducer
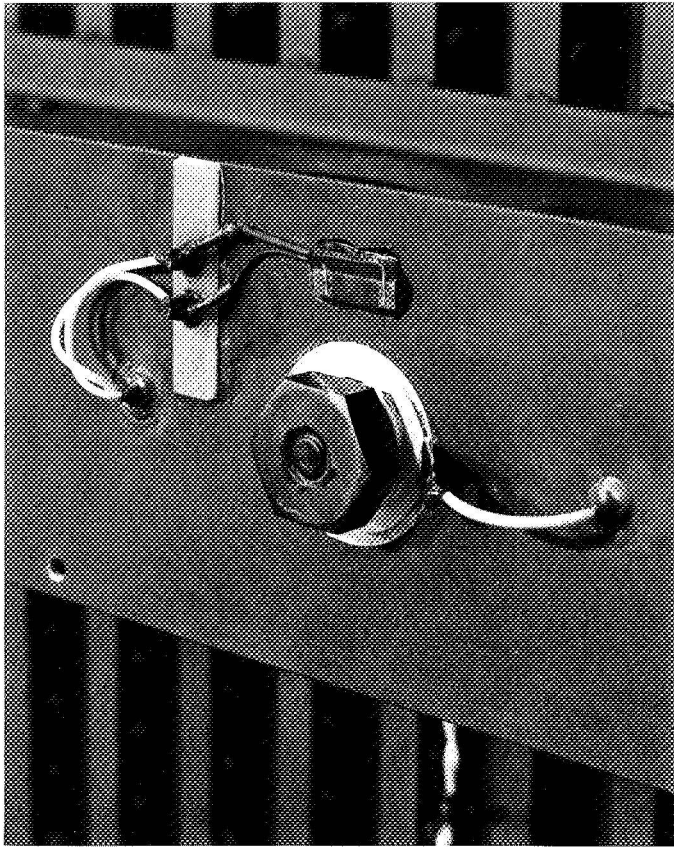
Fig. 7. Typical temperature transducer installation

Fig. 8. Solar panel and spar temperatures as a function of solar intensity

indicated that bonding of the zener to the spar with RTV-40 would result in an acceptable zener temperature-to-power dissipation rate of 7°C/W. Presented in Figs. 8–13 and Table 3 are performance characteristics of the zener regulator as a function of panel performance.

C. Solar Cell

The *Mariner* Venus 67 solar array had 1- × 2-cm *p*-on-*n* (boron-diffused) silicon solar cells with electroless nickel plating and solder-dipped ohmic contacts. These cells were manufactured by Heliotek Corp., Sylmar, Calif. and were procured according to JPL detail and design specifications. To effectively control the quality of the solar cells, JPL provided a source inspector who was required to witness the entire acceptance quality level mechanical and electrical sample testing of each 5000-cell lot.

The solar cells were subjected to additional screening by an independent testing organization, Pan Technical Systems, whose function was to verify, on the same acceptance quality level, the power-output and shape-factor characteristics of each lot of cells and to environmentally

test a 225-cell sample from each lot. This environmental testing was done in accordance with the JPL cell specification and consisted of the following tests: (1) steriliz-ability with ethylene oxide, (2) thermal-vacuum, (3) thermal shock, (4) temperature–humidity, and (5) temperature soak. Electrical performance measurements of all of the cells were required before and after each test. Special tests were also conducted in the JPL photovoltaic laboratory on sample cells from each of the lots to evaluate the effects of temperatures from −20 to 150°C and intensities from 30 to 300 mW/cm² on the electrical performance of the cells. Figure 12 shows a plot of the *Mariner* Venus 67 mean solar cell characteristics before and after filtering and assembly. The data, which are reduced to 100 mW/cm² tungsten data, are intended to show power loss because of assembly.

D. Solar Cell Submodule

1. Design. A solar cell submodule is the smallest sub-assembly of the solar array and consists of seven solar cells and the associated filter covers, filter adhesive, and bus bars. In this design, the seven solar cells were soldered
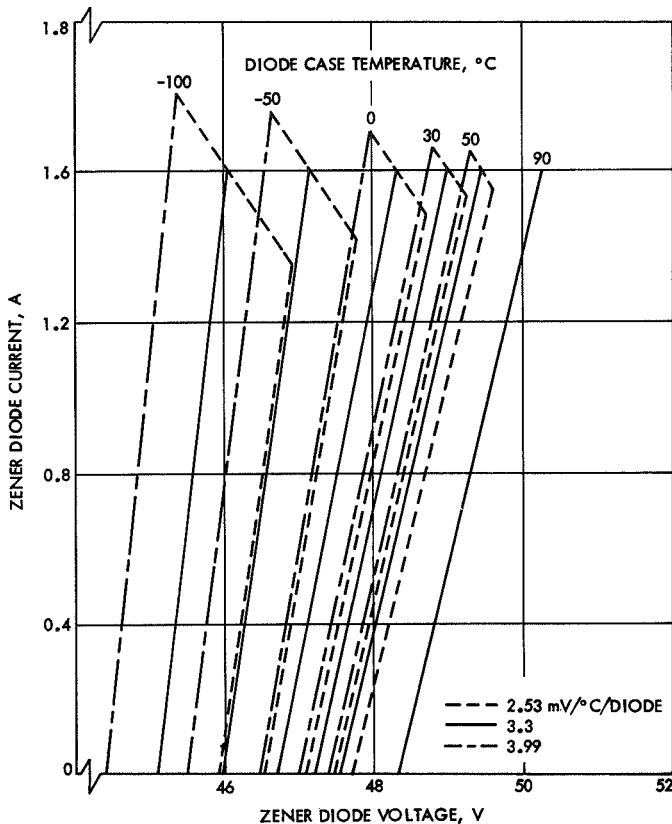
Fig. 9. Zener diode current–voltage characteristics for five diodes per string as a function of diode case temperature

together before assembly of the submodule to the panel (Fig. 13). This design, which was also employed on *Mariner* Mars 1964, provided a means of evaluating the electrical and mechanical characteristics of the individual submodules, thereby improving series string matching and quality assurance inspection techniques, and significantly reducing the amount of work involved in the assembly of thé submodules to the panel. The individual solar cells were electrically interconnected on the *p* side with a 20-mil wire and on the *n* side with a 3-mil-thick ribbon, each of which was gold-plated Kovar. Kovar was employed because of its similar thermal coefficient to the silicon solar cell.

Each solar cell was covered with a glass filter to protect it from low-energy radiation and to aid in temperature control of the cells during flight. These filters were manufactured for JPL by Optical Coating Laboratory, Santa Rosa, Calif. The filter covers were fabricated with a 6-mil-thick Corning 0211 microsheet substrate and a 0.410-μm cutoff filter vacuum deposited on one surface.

A General Electric Co. silicon adhesive, RTV-602, was selected for the cell-filter adhesive. This assembly of filter cover and adhesive had been qualified and successfully flight tested on earlier *Ranger* and *Mariner* programs. To assure the optical and mechanical uniformity and quality of the filters, JPL used source inspection in accordance with the design standard. Batch and in-process control of the RTV-602 adhesive was used to help maintain adhesive quality.

2. Manufacture. Solar cells, filters, and adhesives, after screening by JPL, were fabricated into *Mariner* Venus 67 solar panel submodules by Electro-Optical Systems, Pasadena, Calif. A semi-automatic process involving a tunnel oven was used in soldering the solar cells and Kovar bus bars. Briefly, a tunnel oven is a zone-temperature-controlled oven through which components to be soldered together are automatically conveyed (Figs. 14–18). Oven temperature and conveyor speed may be adjusted as necessary to optimize soldering; it was found that the tunnel oven could be controlled for the time–temperature soldering cycle of a submodule to ensure good bonds and to minimize electrical degradation. The cells were assembled into a machined graphite fixture that correctly positioned the bus bars relative to the cells and fixed the critical maximum and minimum dimensions of the submodule. This technique was used successfully on the *Mariner* Mars 1964 hardware. The *Mariner* Venus 67 submodules were fabricated in a significantly improved version of a tunnel oven that was developed shortly before program initiation by JPL in an advance development effort to investigate improved solar panel fabrication techniques.

E. In-Flight Performance Transducers

Four temperature transducers were used to aid in the evaluation of performance in space of the *Mariner* Venus 67 solar array. In addition, two other temperature-dependent channels were used to evaluate the thermal equilibrium characteristics of the array: (1) the open-circuit voltage cell of the short-circuit current, open-circuit voltage transducer, and (2) the operating points of the solar array when the array was not limited by the zener diode shunts. The temperature transducer outputs were compared with the preflight calibrated open-circuit voltage cell and voltage–current characteristics of the array to help provide solar array temperature data in space.

1. Temperature transducers. The temperature transducer selected for use on the *Mariner* Venus 67 solar array was a small resistive element encased in a thin, electrically insulating mylar jacket approximately 2 mil
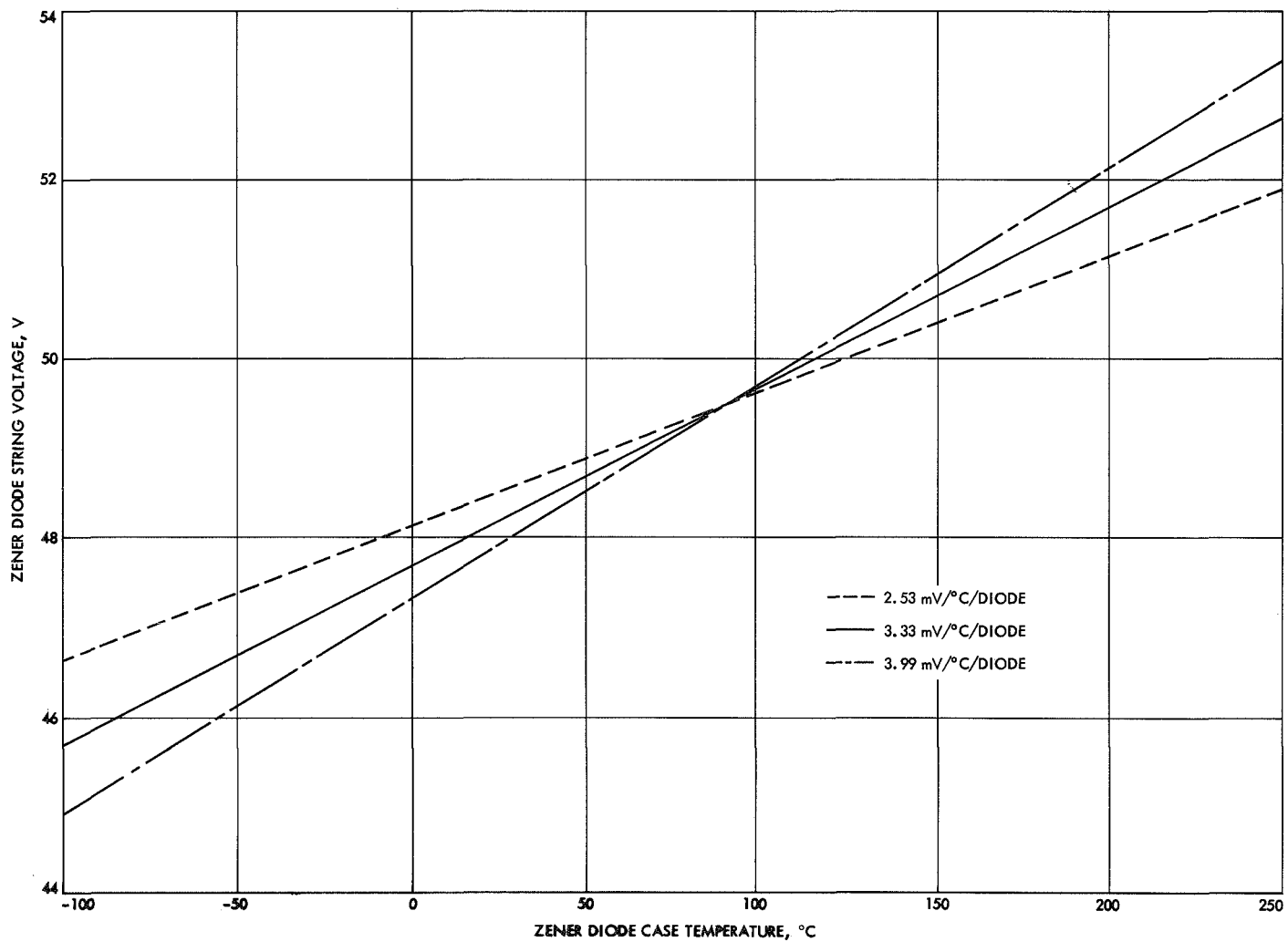
Fig. 10. Zener diode string voltage as a function of diode case temperature
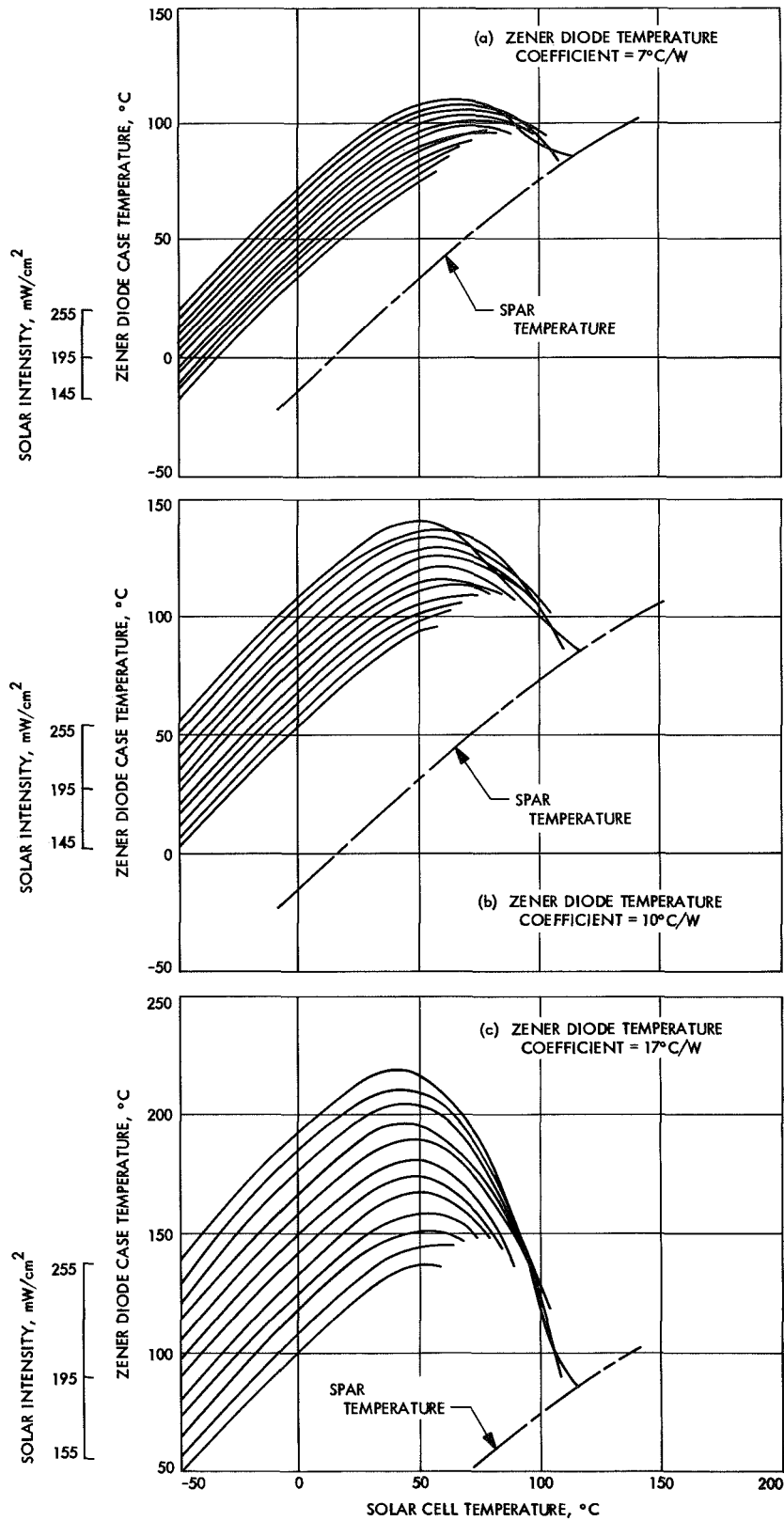
Fig. 11. Zener diode case temperature as a function of solar panel temperature and available power
(no spacecraft load, 105 cells in series)

CELL OR PARAMETER	PRE-ASSEMBLY	POST-ASSEMBLY	POWER LOSS, %
I_{sc}, mA	54.0	49.0	9.3
V_{oc}, V	0.590	0.580	1.5
I2485V, mA	46.5	41.5	10.8
P0485V, mW	22.6	20.1	11.0
MAXIMUM POWER POINT, mW	22.8	20.5	10.0

DATA REDUCED TO mW-TUNGSTEN

CELL TEMPERATURE = 28°C

Fig. 12. Curves of pre- and postassembly average solar cell current and voltage

Fig. 13. Solar cell submodule

Table 3. Zener diode temperature and string voltage as a function of thermal resistance between zener and spar (assuming a minimum spacecraft load of 8 W per section)

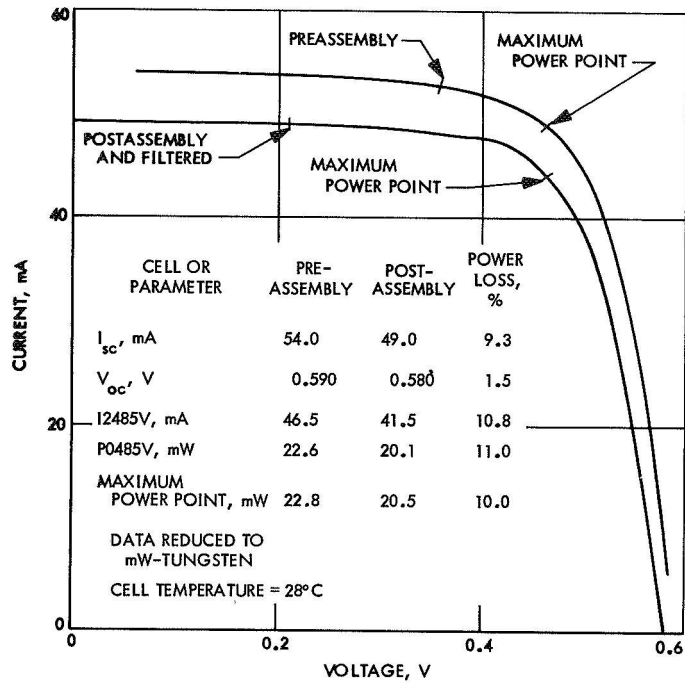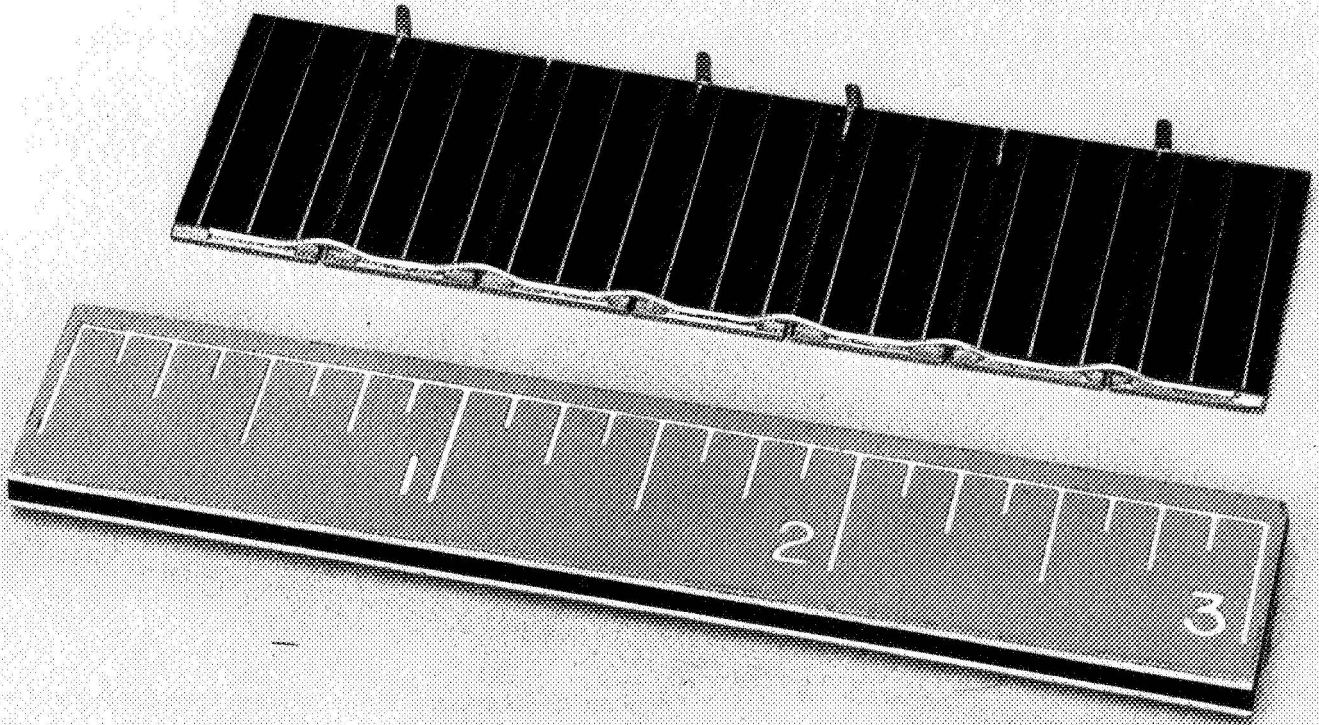| Solar intensity, mW/cm²	Cell temperature, °C	Spar temperature, °C	Section power, W	Power/ diode, W	7°C/W		10°C/W		17°C/W	
					Diode string voltage, V	Diode temperature, °C	Diode temperature, °C	Diode string voltage, V	Diode temperature, °C	Diode string voltage, V
145	−50	−62	31	5.2	−26	46.70	−10	47.08	26	47.94
	0	−14	32.5	5.4	24	47.90	40	48.28	78	49.20
	30	14	32	5.3	51	48.54	67	48.93	105	49.85
	50	32	29	4.8	66	48.90	80	49.25	114	50.08
	57	38	25.5	4.3	68	48.96	81	49.27	110	49.98
155	−50	−62	33.5	5.6	−23	46.78	−6	47.19	33	48.11
	0	−14	35	5.8	27	47.97	44	48.38	95	49.37
	30	14	35	5.8	55	43.64	72	49.06	113	50.05
	50	32	31.5	5.2	69	48.99	84	49.35	121	50.24
	62	43.5	27.5	4.6	75.5	49.14	89.5	49.49	121	50.24
165	−50	−62	36.5	6.1	−19	46.80	−1	47.30	41	48.30
	0	−14	38.5	6.4	31	48.06	50	48.52	95	49.61
	30	14	38	6.3	58	48.72	77	49.17	122	50.26
	50	32	34	5.7	66	48.90	89	49.48	128	50.41
	67	48	27	4.5	80	49.25	93	49.55	125	50.34
175	−50	−62	39.5	6.6	−16	46.95	4	47.43	50	48.52
	0	−14	41	6.8	34	48.15	54	48.63	102	49.78
	30	14	40.5	6.8	61	48.79	82	49.30	129	50.43
	50	32	40.5	6.8	79	49.23	100	49.73	147	50.86
	73	52	24.5	4.1	81	49.27	93	49.55	121	50.24
185	−50	−62	42	7.0	−13	47.00	8	47.52	57	48.69
	0	−14	44	7.3	37	48.21	59	48.75	111	50.00
	30	14	43.5	7.3	65	48.89	87	49.42	137	50.62
	50	32	39.5	6.6	78	49.20	98	49.69	144	50.79
	78	57	24	4.0	85	47.37	97	49.66	125	50.34
195	−50	−62	45.5	7.6	−9	47.10	14	47.67	67	48.93
	0	−14	47	7.8	41	48.30	64	48.87	119	50.20
	30	14	46.5	7.8	68	48.96	92	49.53	146	50.84
	50	32	42	7.0	81	49.27	102	49.78	151	50.96
	75	54	27.5	4.6	86	49.39	100	49.73	132	50.50
	83	62	21	3.5	87	49.41	97	49.66	124	50.32
205	−50	−62	48	8.0	−6	47.19	18	47.75	74	49.11
	0	−14	50	8.3	44	48.39	69	48.99	128	50.41
	30	14	49	8.2	71	49.02	95	49.53	153	51.01
	50	32	44.5	7.4	84	49.35	106	49.87	158	51.13
	75	54	30	5.0	89	49.48	104	49.83	139	50.57
	88	65	17.5	2.9	85	49.37	94	49.60	115	50.10
215	−50	−62	51	8.5	−2	47.29	23	47.88	83	50.32
	0	−14	53	8.8	48	48.49	74	49.11	136	50.57
	30	14	52	8.7	75	49.13	101	49.75	161	51.20
	50	32	47.5	7.9	87	49.41	111	49.98	167	51.34
	75	54	32.5	5.4	92	49.53	108	49.42	146	50.84
	93	69	17	2.8	89	49.48	97	49.66	117	50.15
225	−50	−62	54	9.0	1	47.35	28	48.00	91	49.52
	0	−14	56	9.3	51	48.55	79	49.23	145	50.81
	30	14	55	9.2	78	49.20	106	44.87	170	51.43
	50	32	49.5	8.3	90	49.50	115	50.09	172	51.47
	75	54	34	5.7	94	49.60	111	49.98	150	50.43
	98	73	11.5	1.9	86	49.39	92	49.53	106	49.87

Table 3 (contd)

Solar intensity, mW/cm²	Cell temperature, °C	Spar temperature, °C	Section power, W	Power/diode, W	7°C/W		10°C/W		17°C/W	
					Diode temperature, °C	Diode string voltage, V	Diode temperature, °C	Diode string voltage, V	Diode temperature, °C	Diode string voltage, V
235	−50	−62	56.5	9.4	4	47.42	32	48.09	98	49.69
	0	−14	59.5	9.9	56	48.67	85	49.37	155	51.05
	30	14	58	9.7	82	49.30	111	49.98	178	51.61
	50	32	52.5	8.8	93	49.56	120	50.20	181	51.68
	75	54	36	6.0	96	49.63	114	50.07	156	51.08
	103	78	6.5	1.1	85.5	49.38	89	49.48	96	49.63
245	−50	−62	59.5	9.9	8	47.51	37	48.21	107	49.90
	0	−14	62.5	10.4	59	48.75	90	49.50	163	51.25
	30	14	60.5	10.1	85	49.37	115	50.09	185	51.78
	50	32	54.5	9.1	96	49.63	123	50.28	186	51.80
	75	54	38	6.3	98	49.69	117	50.14	162	51.22
	108	82	0	0	82	49.29	82	49.29	82	49.30
255	−50	−62	63	10.5	12	47.61	43	48.35	117	50.15
	0	−14	65	10.8	62	48.81	94	49.60	170	51.43
	30	14	63.5	10.6	88	49.44	120	50.20	194	52.00
	50	32	57	9.5	99	49.71	128	50.40	194	52.00
	75	54	39	6.5	100	49.73	119	50.19	165	51.30
	100	75	6	1.0	82	49.29	85	49.37	92	49.55
	115	86	0	0	86	49.39	86	49.39	86	49.39

thick. The transducer, a Trans-Sonics, Inc., type T4242, exhibits a relatively linear resistance-vs-temperature characteristic in the range from +300 to −300°F.

These transducers were procured and screened by JPL and supplied as government-furnished equipment to the solar array manufacturer. Three transducers were bonded to each panel, one in the center of the panel, one under the I_{sc}–V_{oc} transducers, and one on the spar of the structure close to the zener diode. In flight, only four temperature transducers were monitored: the center unit on panels 4A1 and 4A5, and the I_{sc}–V_{oc} transducer and spar units on panel 4A5. Trans-Sonics, Inc. epoxy cement resin 2369 and catalyst 2370 were used to bond the transducer directly to the panel. The lead-in wires were also bonded to the panel substrate to minimize losses from heat conduction. On completion of the bonding, Laminar X-500 paint was applied to the transducer and to the area around it.

2. Short-circuit current, open-circuit voltage transducers. Each solar panel included a short-circuit current, open-circuit voltage transducer to aid in the evaluation of array performance during flight. The transducer was composed of three 1- × 2-cm *Mariner* Venus 67 solar cell assemblies; two of the assemblies were instrumented to monitor their short-circuit current outputs, and the remaining cell was instrumented to monitor its open-circuit voltage. One of the two short-circuit current cells used in the transducer was bombarded with electrons to approximately a 10^{15} electron/cm² flux level before assembly. This radiation dose degraded the short-circuit current output of the cell approximately 50%, which rendered the cell relatively insensitive to further radiation degradation. Results of the bombardment provided an indication of the relative space radiation damage to the cell; performance of the bombarded cell was compared with that of the short-circuit current cell not subjected to preflight radiation damage.

The I_{sc}–V_{oc} transducer assembly was fabricated by JPL and supplied to the array manufacturer. The transducer was located at the bus end of the panel near the panel centerline. Preflight calibration of the I_{sc}–V_{oc} transducer cells required intensity and temperature calibration under 2800°K tungsten illumination and sunlight at the JPL Table Mountain test facility. The cells were standardized on a JPL standardization balloon flight; the cells were flown at 80,000 ft and data on the output of the cells in sunlight was telemetered to earth. These cells were later recovered and incorporated into the I_{sc}–V_{oc} transducer.
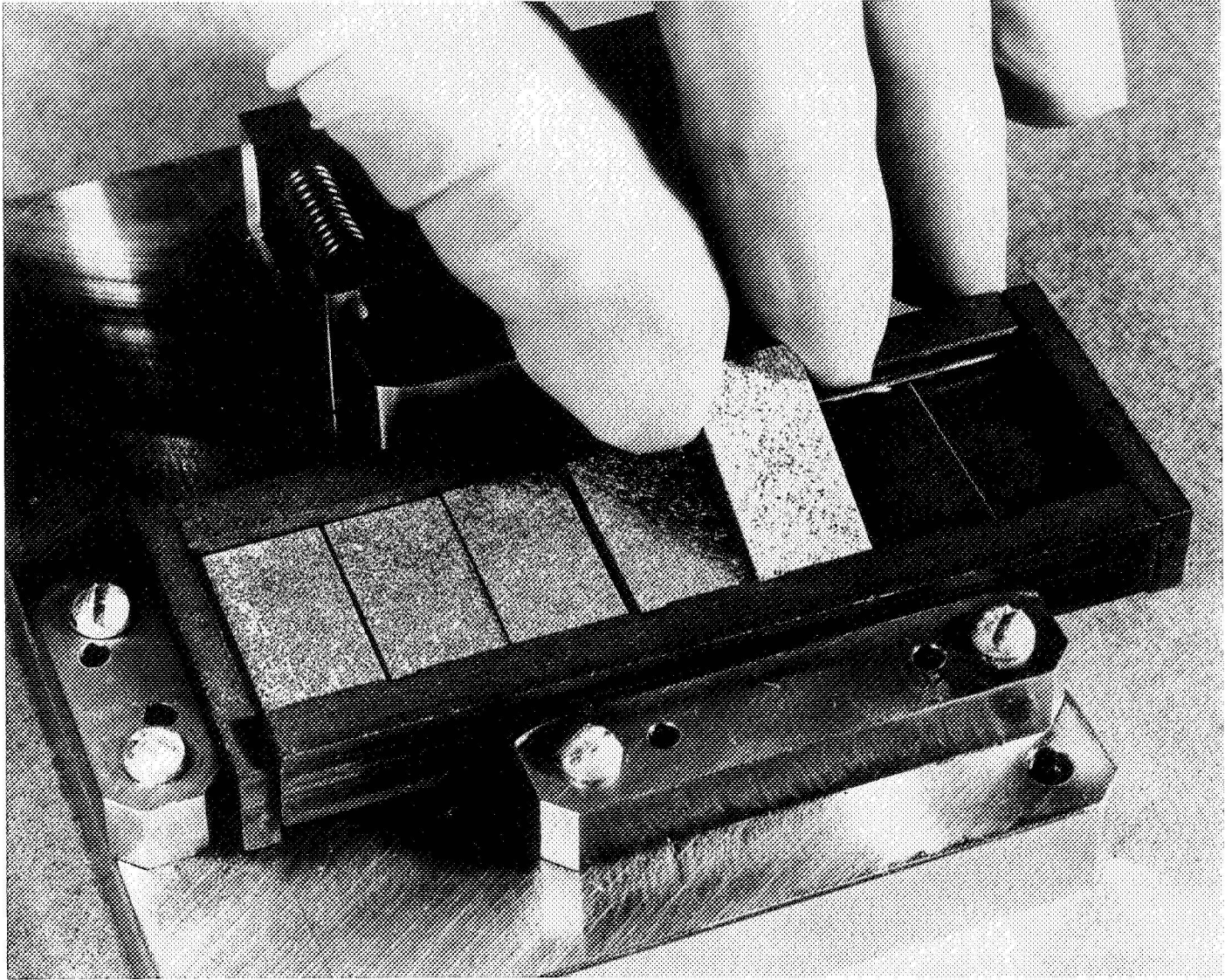
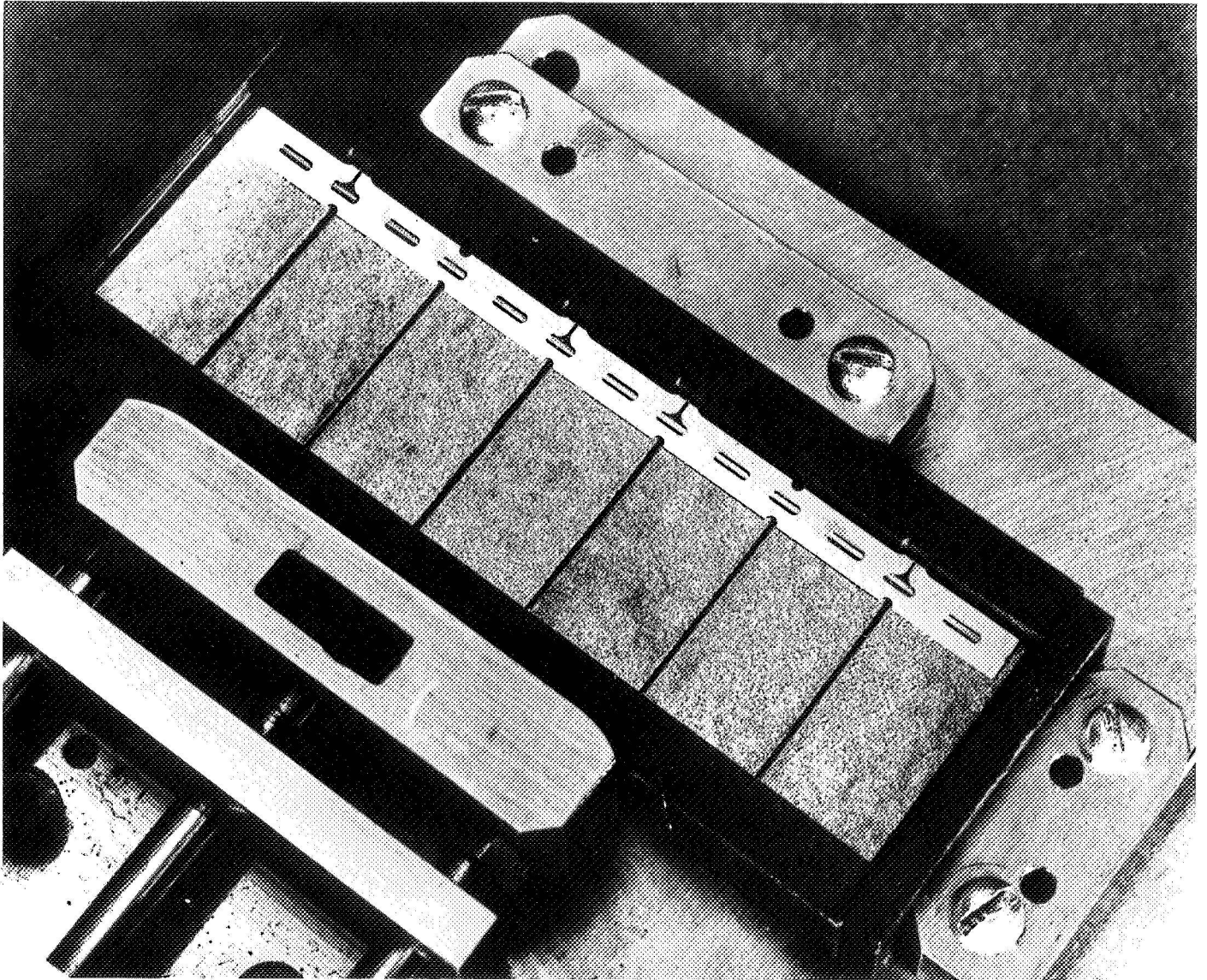Fig. 14. Solar cell submodule being assembled into soldering fixture

Fig. 15. Solar cell submodule in soldering fixture before entering tunnel oven
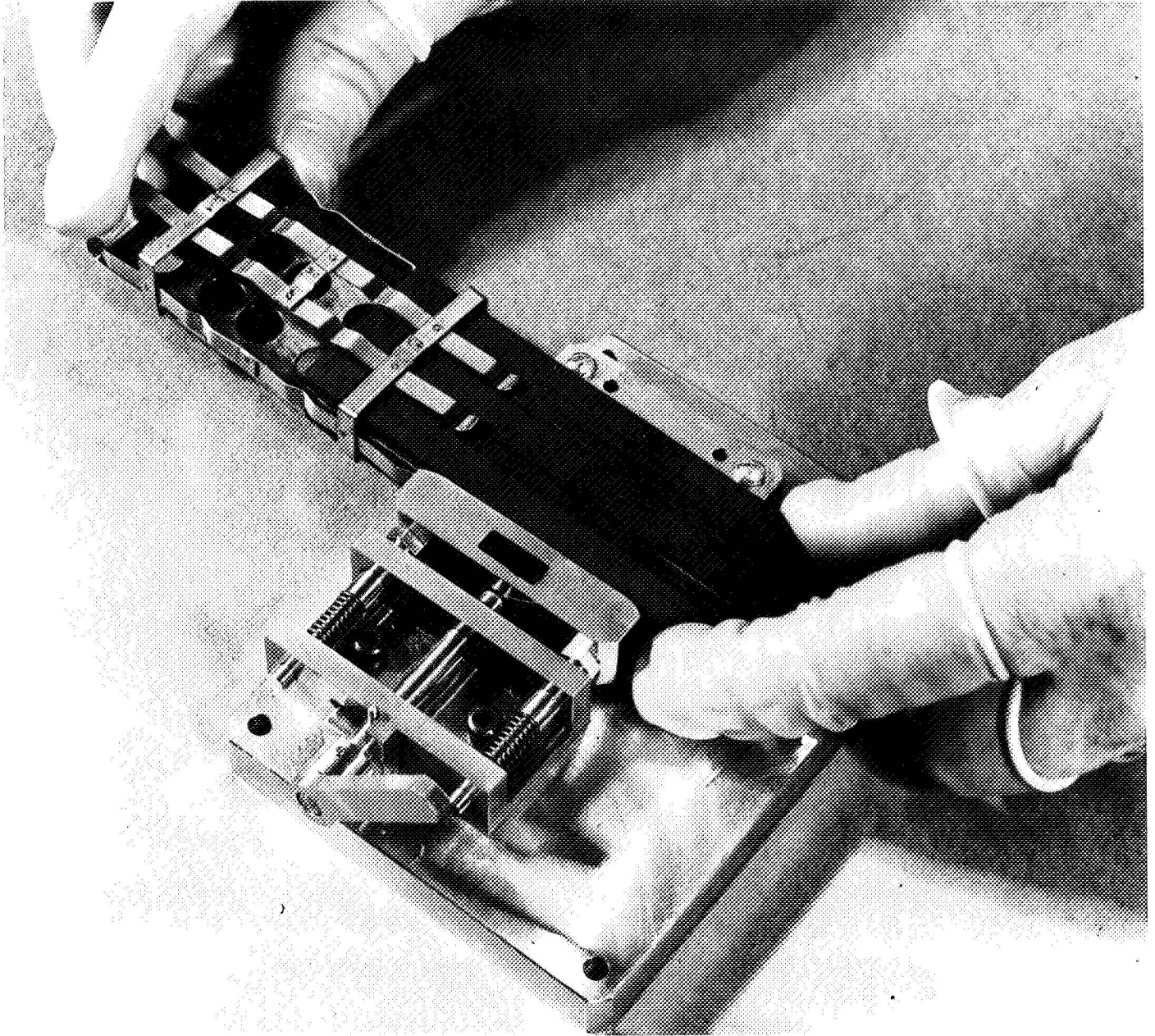
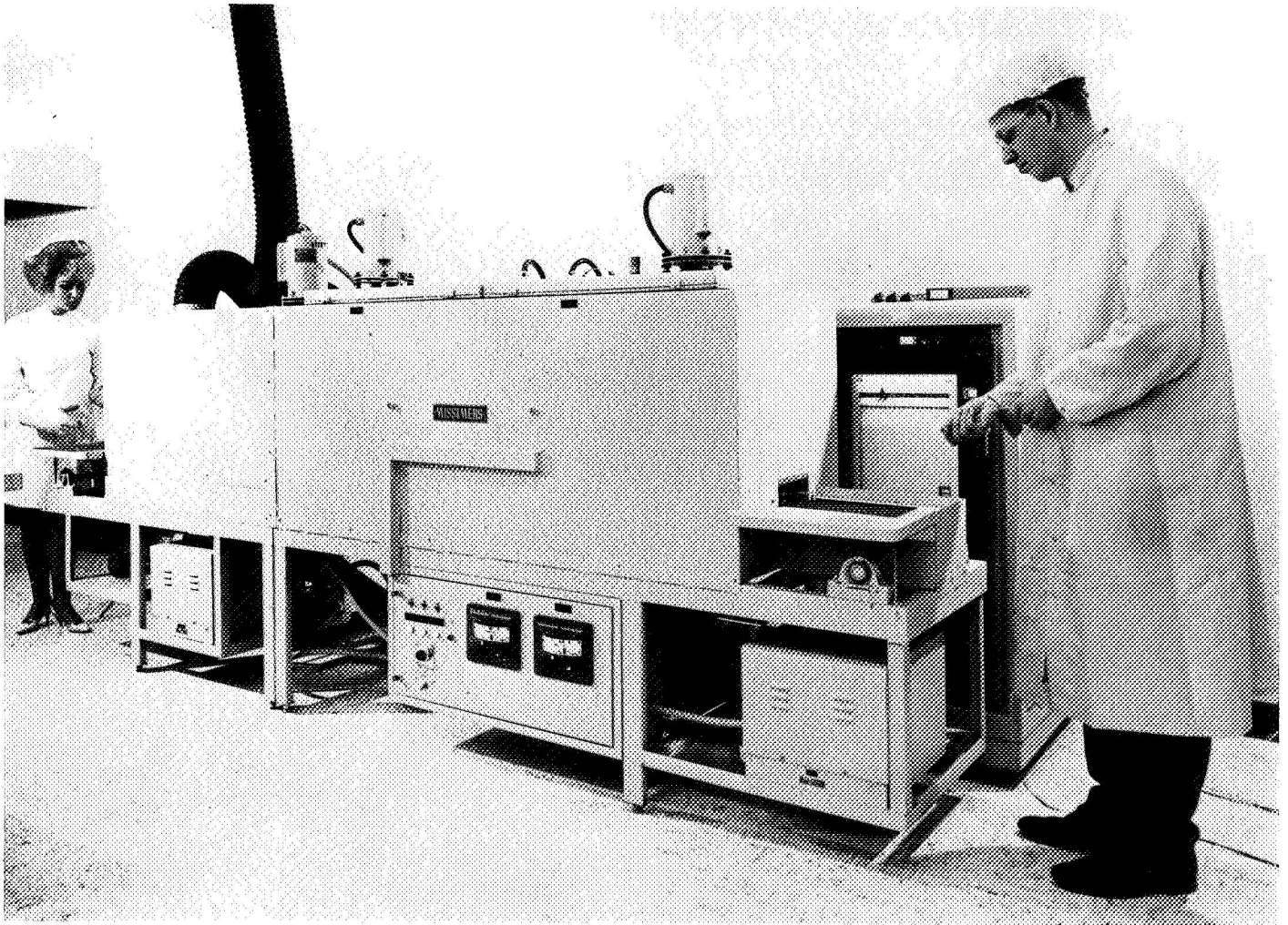Fig. 16. Solar cell submodule soldering fixture in final assembly stage

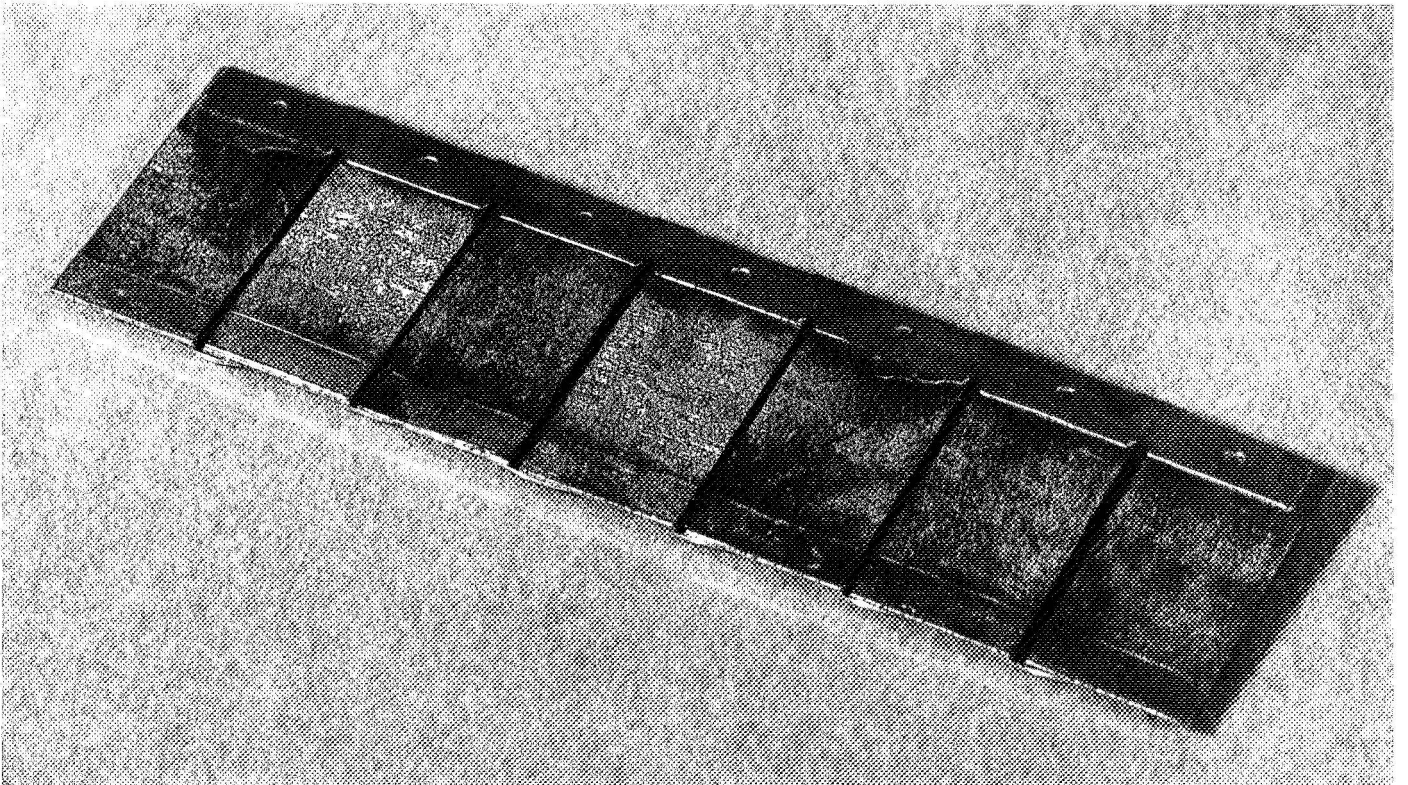Fig. 17. Tunnel oven used in solar cell submodule fabrication

Fig. 18. Solar cell submodule back surface after soldering in tunnel oven

III. Assembly

Solar cell submodules, substrates, zener diodes, and transducers procured and screened by JPL were supplied to Electro-Optical Systems for assembly into solar panels. One type approval and six flight panels were fabricated and tested for this program. An elaborate quality control and manufacturing process control system was established, which required frequent in-process inspection by both Electro-Optical Systems quality assurance and JPL resident inspectors.

The submodules were bonded to the front surface of the panel with General Electric RTV-40 silicon adhesive and connected in a matrix of 14 cells in parallel and 105 cells in series in each electrical section.

There were 1470 solar cells in each of the three electrical sections, 4410 cells in each of four panels, and 17,640 cells in the *Mariner* Venus 67 vehicle.

Bondable Teflon wire (22 gage) was used to harness the solar cell sections to the panel connector, a Bendix JC 004 18-32S. The harness was routed along both inboard edges of the substrate spars and was supported with Teflon cable clamps. All feedthrough holes for connection of the harness to the submodules were at the bus end of the panel. Connecting wires were routed from the main bundle attached to the spars, across the panel, and through these holes. In all cases, the wire was protected from damage at the hole by a Teflon grommet.

To minimize the requirement for feedthrough holes in the panel and reduce mechanical stress associated with the attachment of the harness cable directly to the submodules, a conformal-coated printed circuit board was developed. The circuit boards provided all the intersubmodule redundant wiring required and were bonded to the cell surface of the substrate with RTV-40.

IV. Testing

A. Environmental Qualification Testing

Qualification of a *Mariner* Venus 67 solar array required successful completion of a type approval test program that included vibration, thermal-vacuum, acoustic noise, and humidity. All solar panels that were to be designated flight hardware were required to successfully complete a vibration and thermal-vacuum flight approval test program. Evaluation of the effects of the test on a solar panel was based on: (1) a comparison of the nor-

malized electrical performance characteristics made in sunlight before and after each test at the JPL Table Mountain test facility, and (2) a 10× microscopic inspection of all the panel assemblies and solder connections. Test levels and acceptance criteria were specified in JPL solar panel test approval and flight approval environmental test specifications.

The solar panel successfully passed the type approval vibration and acoustic tests; however, during the thermal-vacuum test that was conducted in the JPL 10-ft solar simulator, a loss of electrical power to the simulator occurred. Prior to this time, the panel had been subjected to two thermal shocks simulating midcourse maneuvers at various distances from the sun (panel temperatures of 130 and 165°F) and was exposed to a 100-h soak at 280°F. The failure of the light source power occurred after 85 h of the high temperature soak. This failure caused a severe thermal shock to be induced into the panel. An electrical and mechanical inspection of the panel after removal from the chamber revealed that 16% of the solar cells showed p-contact delamination and that the electrical power output capability of the panel had decreased approximately 27%.

An extensive testing program was conducted to provide additional information for purposes of evaluating the mechanism and mode of failure. Twelve 1-ft² sample solar panels were fabricated and were tested under varying thermal-shock and thermal-soak conditions. The resulting data indicated that the type approval panel would have successfully survived the thermal vacuum tests with probably no broken cell contacts if the power to the solar simulator had not failed. No cell contact failures or design inadequacies were revealed in subsequent real-time life testing of two 1-ft² solar panels in a thermal-vacuum environment similar to that anticipated for the *Mariner* Venus 67 mission through 30 days after encounter.

It was anticipated that all flight solar panels would be qualified as individual subassemblies before delivery to the Spacecraft Assembly Facility and before spacecraft flight approval testing. However, because the panels were latched at the ends when mounted on the spacecraft and, therefore, supported and acted upon one another, it was found to be difficult to vibration-test individual solar panels with confidence. It was also determined that there could be significant variations in the response from panel to panel and there was a constant concern of overtesting. Midway through the flight approval vibration test program, the decision was made to forego individual panel vibration qualification and to use the spacecraft vibration

test to certify the mechanical integrity of each panel. No difficulties or abnormalities were encountered in this connection in the remainder of the program.

B. Electrical Performance Testing

All electrical performance tests of *Mariner* Venus 67 solar panels were conducted at the JPL Table Mountain test site located 7000 ft above sea level, near Wright-wood, Calif. The panels were oriented normal to sunlight and the current–voltage characteristic of each of the electrical sections was measured in the ambient temperature–humidity environment. The relative space intensity of the sunlight at the time of testing was monitored by a balloon flight standardized solar cell that had spectral response characteristics similar to those of the solar cells on the panel. The temperature of the panels was determined from the open-circuit voltage output normalized to a sun intensity in space of 135 mW/cm^2 and compared to calibration curves relating voltage and temperature. The equations employed to reduce solar panel data to space conditions are:

$$I_2 = I_1 + I_{sc_1}\left(\frac{L_2}{L_1} - 1\right) + \alpha(T_2 - T_1)$$

$$V_2 = V_1 - \beta(T_2 - T_1) - \Delta I_{sc}R_s - K(I_2 - T_1)I_2$$

$$\Delta I = \Delta I_{sc} = I_{sc_1}\left(\frac{L_2}{L_1} - 1\right) + \alpha(T_2 - T_1)$$

$$P_2 = I_2 V_2$$

where

$$\alpha \equiv \frac{dI_{sc}}{dT}\bigg| \text{ intensity constant}$$

$$\beta \equiv \frac{dV_{oc}}{dT}\bigg| \text{ intensity constant}$$

$I_1 =$ reference current coordinate

$V_1 =$ reference voltage coordinate

$I_{sc_1} =$ short-circuit current of the reference data

$I_2 =$ extrapolated current coordinate

$V_2 =$ extrapolated voltage coordinate

$L_1 =$ reference incident solar intensity

$L_2 =$ equivalent solar intensity to be investigated

$T_1 =$ reference cell temperature

$T_2 =$ cell temperature to be investigated

$R_s =$ panel effective series resistance

$K =$ series resistance correction function for temperature

$\alpha =$ short-circuit current temperature coefficient

$\beta =$ open-circuit voltage temperature coefficient

The uncertainty of predicting the performance characteristics of a solar panel in space on the basis of Table Mountain measurements was assumed to be 8%. A breakdown of the causes for this uncertainty factor is shown in Fig. 19. These factors are treated here as dependent variables.
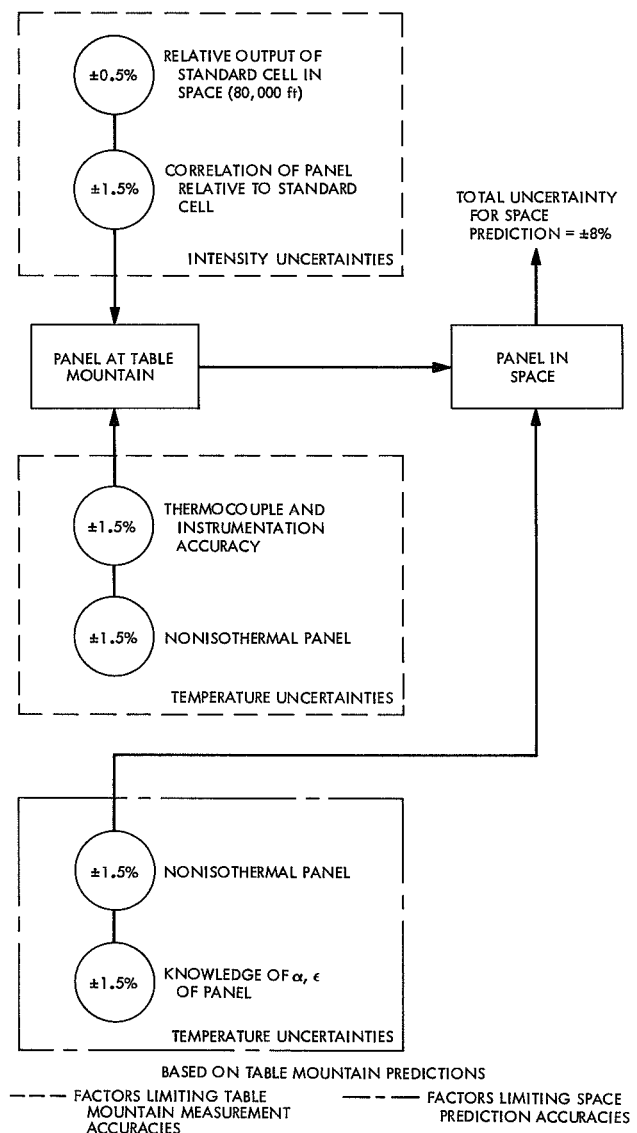

Fig. 19. Prediction capability for a solar panel in space at some heliocentric distance

Table 4. Summary of electrical performance testing data, *Mariner* Venus 67 solar panels[a]

Panel	Section	Power (maximum power point), W	Voltage (maximum power point), V	Short-circuit current, A	Open-circuit voltage, V
003 (spare)	A	32.59	43.74	0.833	56.73
	B	33.31	45.26	0.832	56.73
	C	33.42	43.88	0.849	56.64
004 (spare)	A	34.00	44.84	0.857	56.69
	B	33.80	44.51	0.851	56.69
	C	33.56	44.96	0.847	56.68
005 (4A5)	A	34.02	44.73	0.844	56.69
	B	33.90	45.03	0.848	56.69
	C	34.01	45.42	0.850	56.69
006 (4A7)	A	33.55	44.16	0.841	56.67
	B	33.67	44.84	0.843	56.69
	C	34.00	44.42	0.848	56.69
007 (4A1)	A	34.09	44.56	0.852	56.69
	B	34.17	45.29	0.854	56.69
	C	34.05	44.93	0.854	56.67
008 (4A3)	A	34.04	45.22	0.845	56.69
	B	34.12	45.73	0.849	56.69
	C	34.16	44.42	0.850	56.69

[a]Data reduced to 135 mW/cm² and 58°C.

A summary of the electrical performance of the six *Mariner* Venus 67 flight panels is presented in Table 4. The data indicate that the panels (particularly the four flight panels) were relatively uniform.

V. Performance Predictions

A. Thermal Characteristics

Because the design of the *Mariner* Venus 67 solar array is very similar in construction and materials to that of the *Mariner* Mars 1964 solar array, it was felt that the preflight and flight temperature data and analysis would be directly applicable in most cases. It was also expected that a lengthwise temperature gradient caused by the influence of the bus would be negligible in view of the distance between the inboard edge of the cells and the bus. Presented in Figs. 20–25 are the predicted flight temperature conditions of the array including: (1) the anticipated temperature rise on the array during encounter because of the Venus albedo, and (2) the transient conditions predicted for the array during a nominal worst-case type of midcourse maneuver. *Mariner* Mars

1964 flight data generally supported the fact that this array could be nominally described as following a simple flat-plate thermal analysis in which the area of the front surface of the panel effectively equals the area of the rear surface.

B. Electrical Characteristics

The predicted preflight electrical characteristics of the array are shown in Figs. 26–30. It was calculated that incident solar intensity at the time of launch would be 135 mW/cm² and that the resulting temperature, based on *Mariner* Mars 1964 data, would be 56°C. The relative effect of a 7°C lower temperature on the power output capability of the solar array is shown in Fig. 29. From preflight measurements it was determined that an undegraded *Mariner* Venus 67 solar array should have a power temperature correction factor of approximately 0.32%/°C. Maximum power output as a function of heliocentric distance for an undegraded *Mariner* Venus 67 solar array is shown in Fig. 26. It can be seen in Fig. 28 that, because of the zener diode limiting during the early stages of the flight, the output voltage of the array will be determined by the zener diodes. Assuming nominal performance and
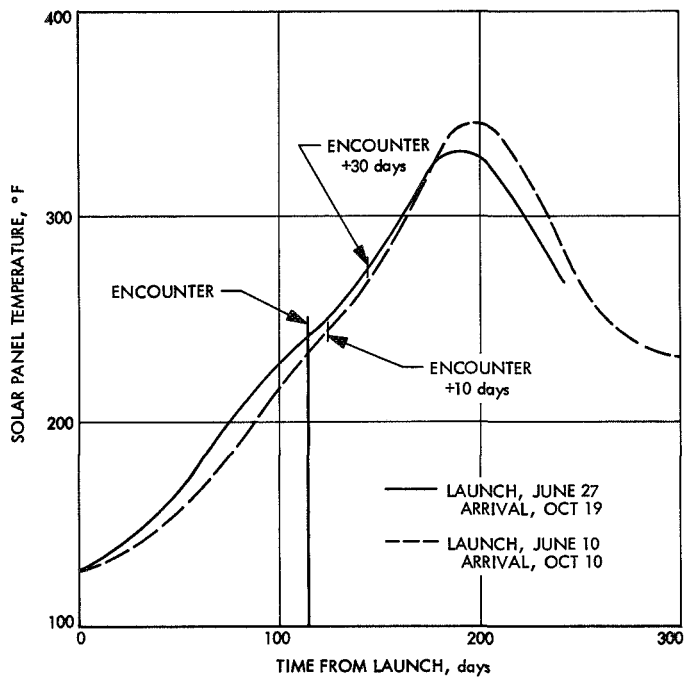
Fig. 20. Predicted solar panel temperature for
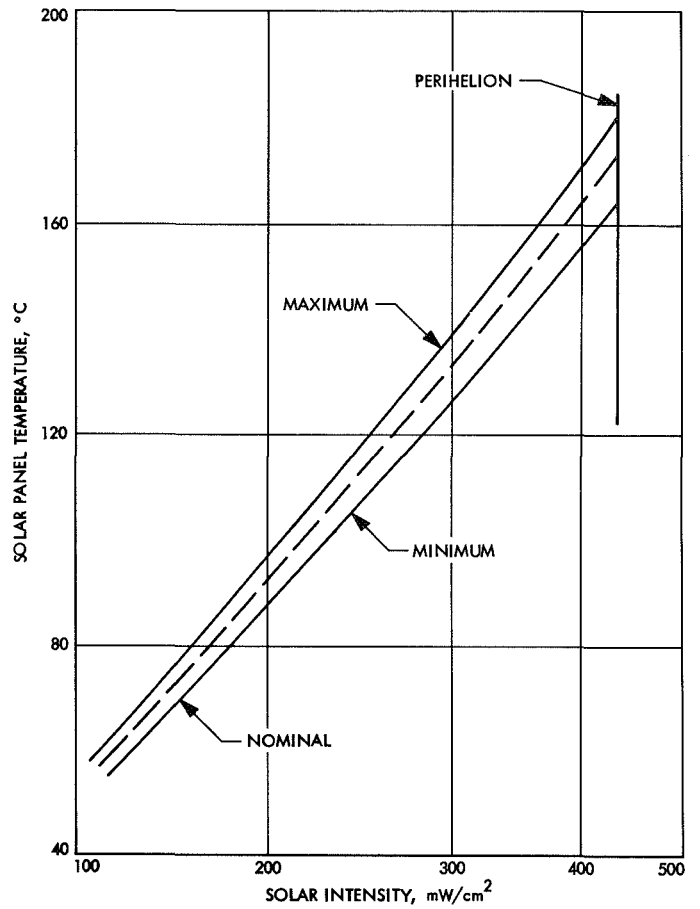*Mariner* Venus 67 mission

Fig. 21. Predicted solar panel temperature vs solar
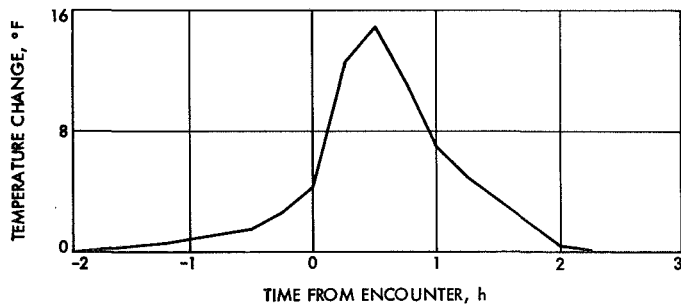intensity for *Mariner* Venus 67 mission

Fig. 22. Predicted solar panel temperature rise
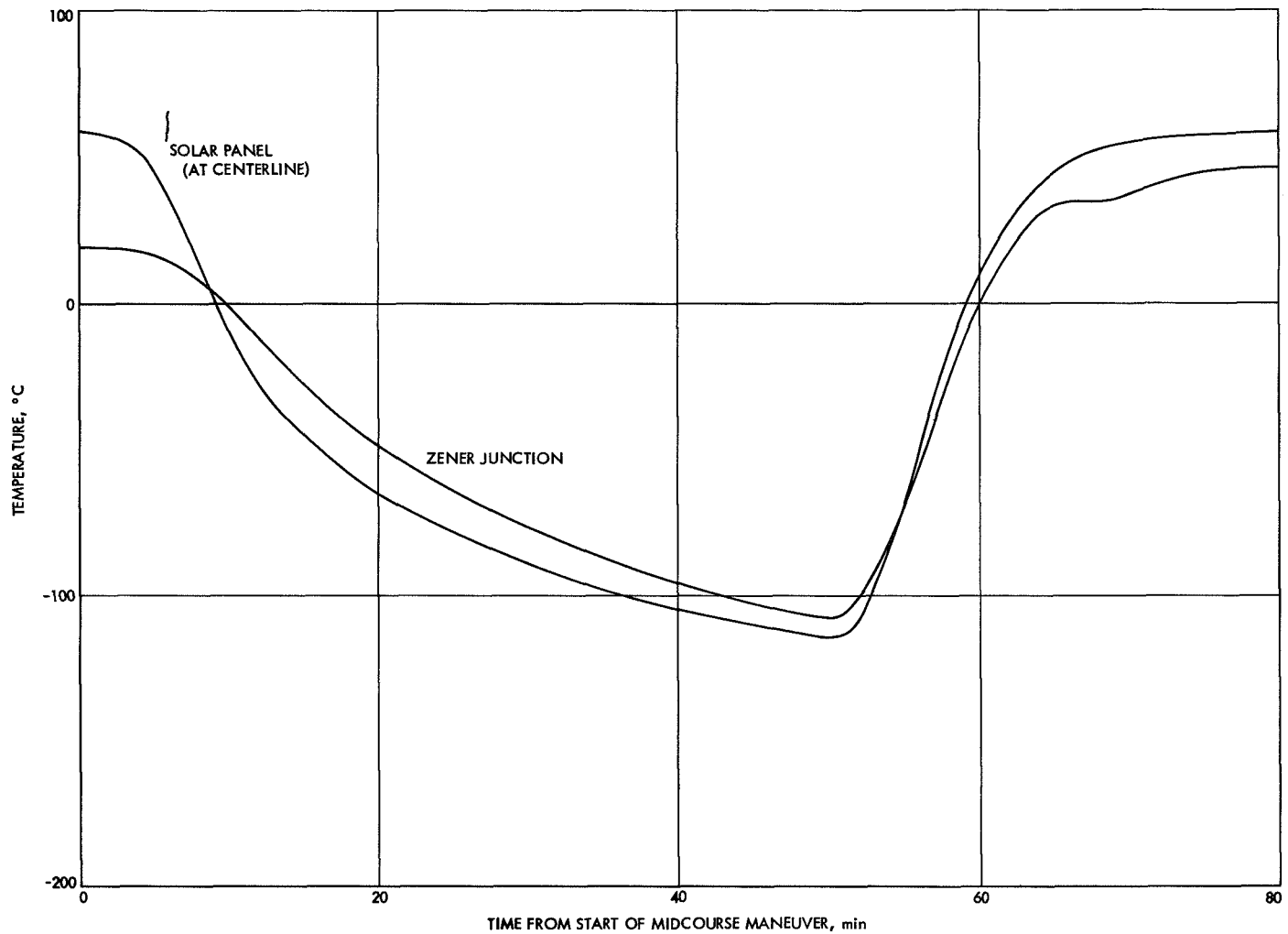during Venus encounter

Fig. 23. Predicted solar panel temperature profile during *Mariner* Venus 67 midcourse maneuver
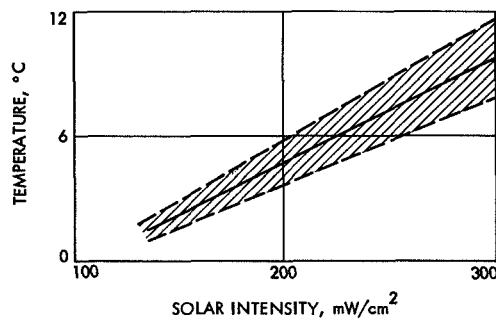

Fig. 24. Predicted temperature gradient through the solar panel as a function of solar intensity between Venus and earth
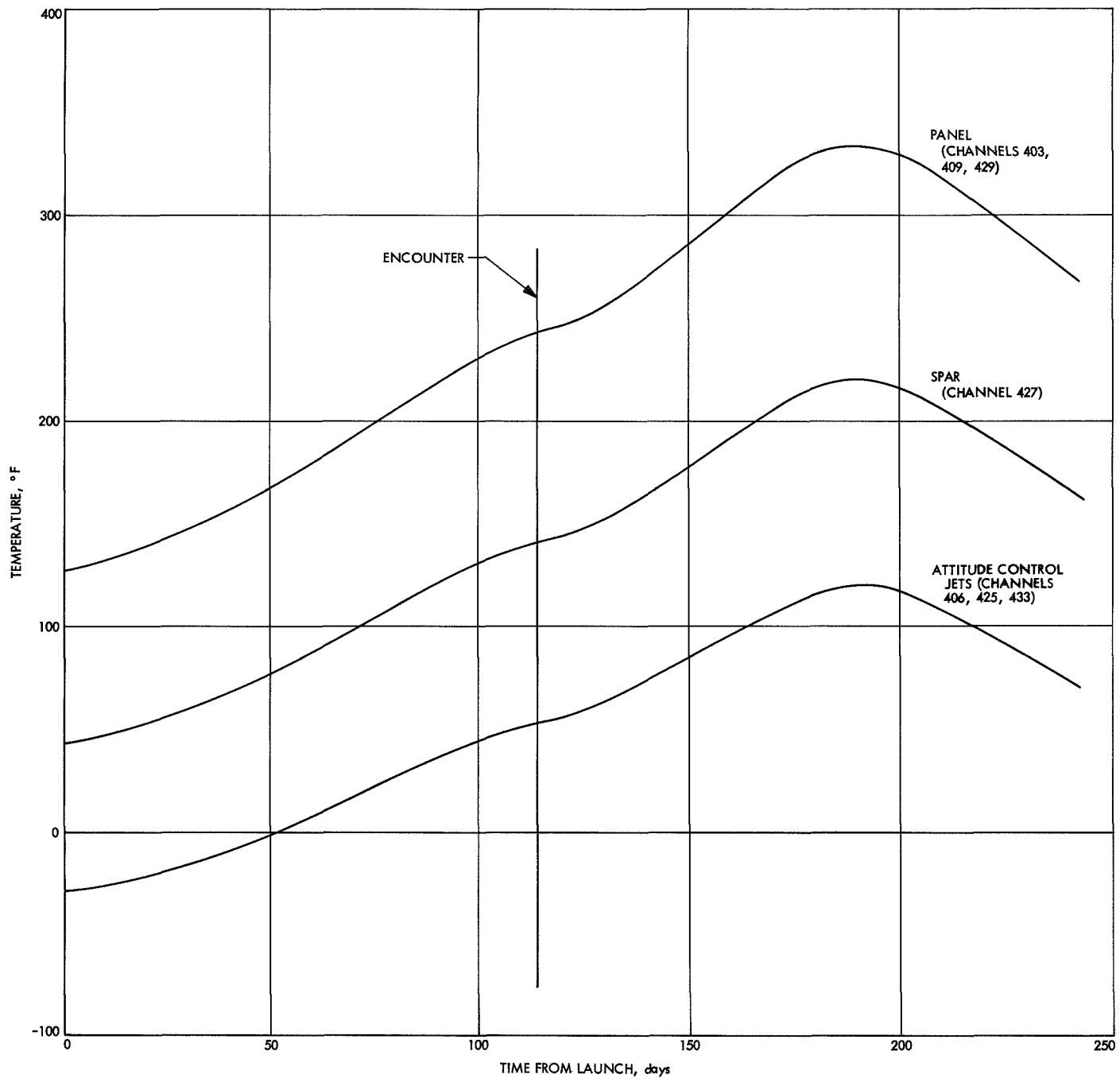
Fig. 25. Predicted solar array temperatures during *Mariner* Venus 67 mission
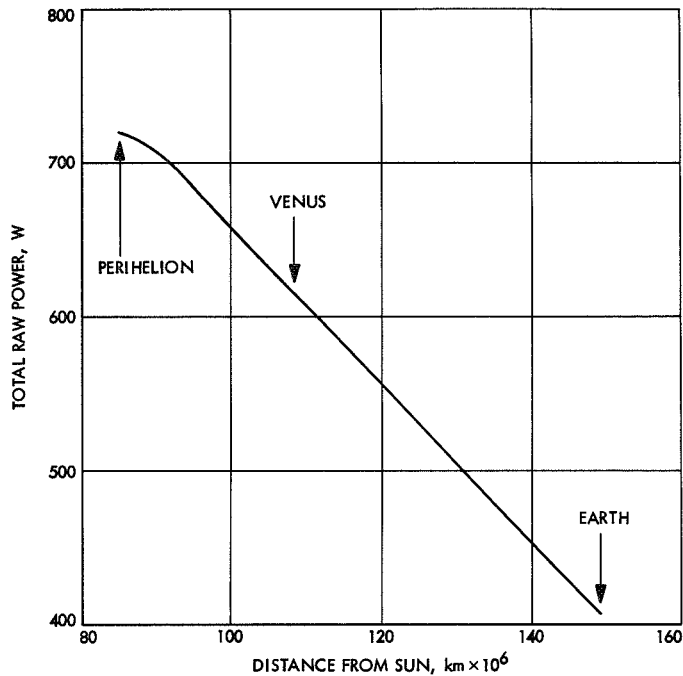
Fig. 26. Total undegraded spacecraft solar panel peak
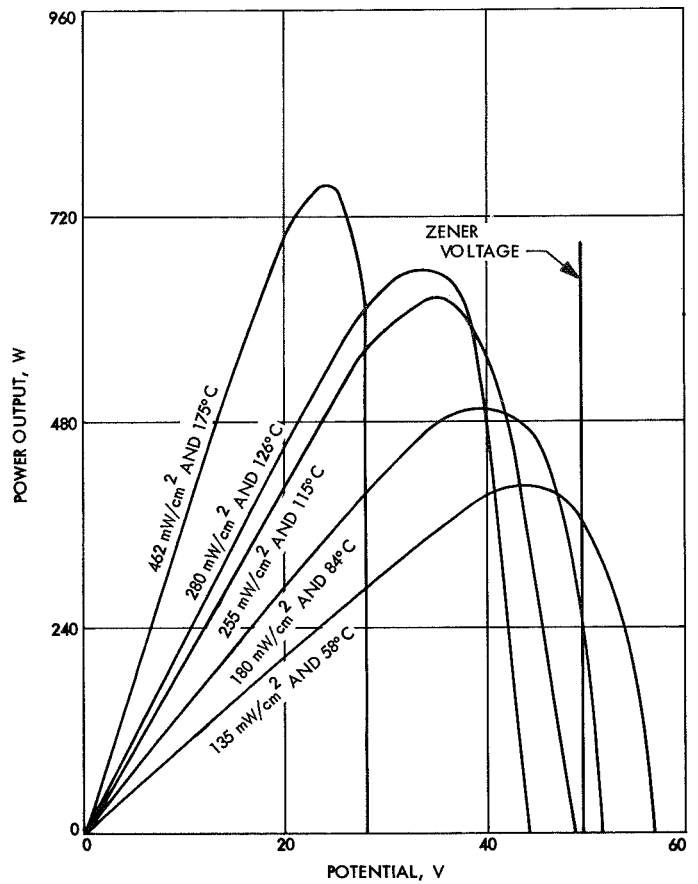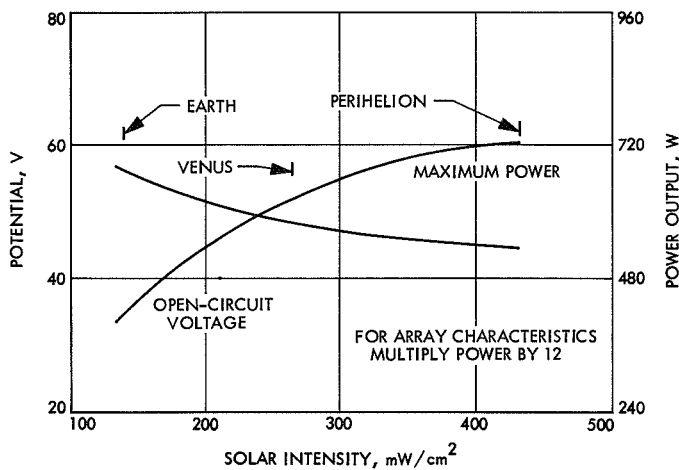raw power vs heliocentric distance

Fig. 27. Variation of solar panel section performance
with solar intensity
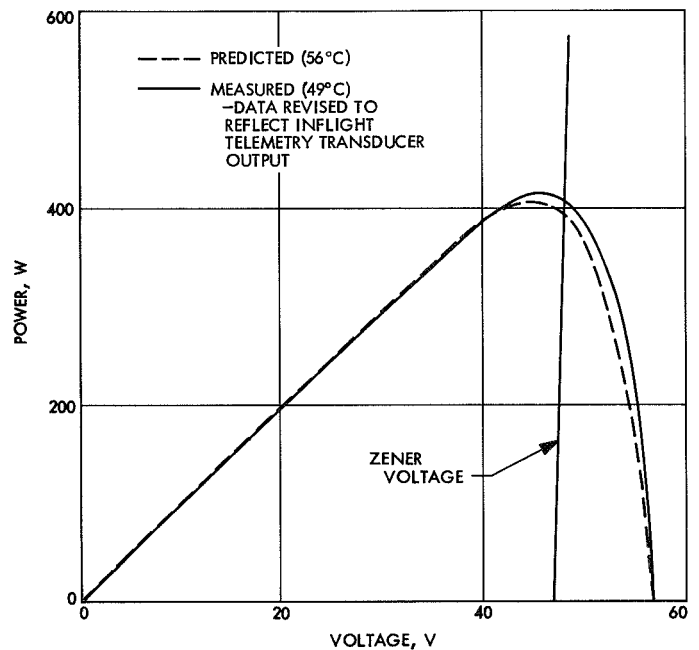
Fig. 29. Predicted and measured power vs voltage,
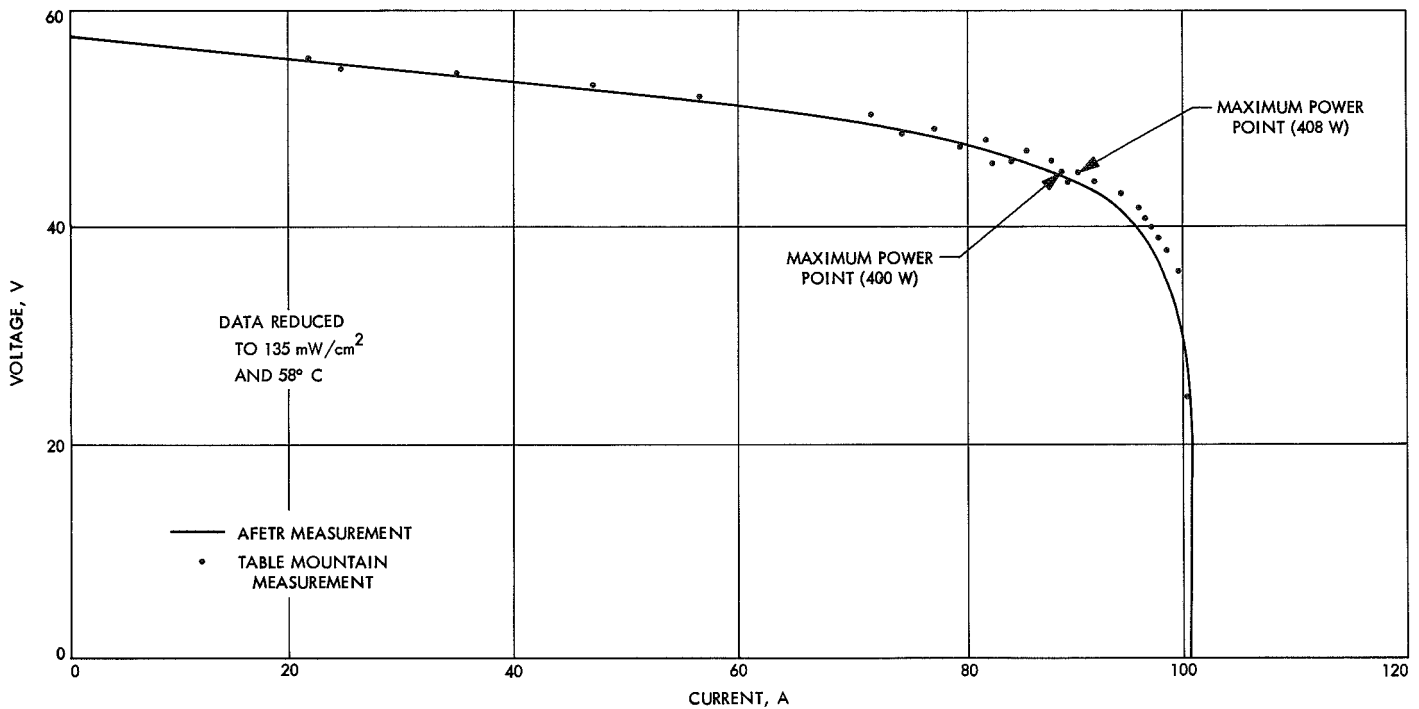*Mariner* Venus 67 solar array

Fig. 28. Solar panel power vs voltage for
various conditions

MAXIMUM POWER
POINT (408 W)

MAXIMUM POWER
POINT (400 W)

DATA REDUCED
TO 135 mW/cm^2
AND 58° C

40

20

VOLTAGE, V

——— AFETR MEASUREMENT
• TABLE MOUNTAIN
MEASUREMENT

0
0   20   40   60   80   100   120
CURRENT, A

Fig. 30. Comparison of AFETR and Table Mountain test station data, *Mariner* Venus 67 solar array current and voltage

a cruise spacecraft load of 200 W, it is anticipated that the zeners will determine the voltage output until a panel temperature of approximately 80°C (176°F) is reached. Prior to this time, the panel output voltage should vary only slightly. After this period, larger variations should be expected.

Prior to launch, a last electrical check of the solar array was made at the Air Force Eastern Test Range (AFETR). The AFETR data were normalized to space sunlight conditions and the output was compared to reduced data of the solar panels when last measured at Table Mountain. These data (Fig. 30) show agreement to within 2%. Considering the AFETR test conditions and limitations of resolving data, it is felt that these results support the conclusion that the panels appeared undamaged or undegraded and ready for flight.

VI. In-Flight Performance Summary

The *Mariner* Venus 67 solar array apparently performed satisfactorily. There were, however, three parameters for which initial values were other than the predicted nominals. The solar panel temperature was approximately 7°F lower than predicted and the short-circuit current and radiation-resistant short-circuit current

cells of the $I_{sc}-V_{oc}$ transducer produced approximately 4% more output than predicted.

Investigations were initiated to determine the significance of these discrepancies. The temperature offset was found to have been caused by the additional power that was dissipated by the zener diodes. The diodes were effectively loading the panel close to the panel maximum power point, and the solar array was converting solar energy to electrical energy at a rate greater than 9 W/ft^2; this compares with only 3 W/ft^2 then required by the spacecraft load. The difference of 6 W/ft^2, together with the poor thermal path the additional power dissipated in the diodes would have in providing heat back to the panel region around the temperature transducer, accounts for most of the offset. The prelaunch prediction was based on only the 3 W/ft^2 dissipation by the spacecraft.

The $I_{sc}-V_{oc}$ transducer output difference was traced to the calibration technique used to standardize the cells. The technique used to perform the standardization required that different load resistors be used on the balloon and on the spacecraft. The sizes of these resistors are relatively small (1.00 and 0.175 Ω, respectively); small variations in these resistors, in addition to handling and interconnection techniques, could well account for this

variation. It had been planned that immediately prior to shipment, the transducer on the solar panel would receive a final calibration at Table Mountain. However, because of poor weather, the calibration was not performed, and the need for absolute calibration of the transducer was not considered important enough to warrant delaying shipment.

Solar array performance during the mission was apparently nominal; the data are tabulated in Table 5. The $I_{sc}-V_{oc}$ transducer performance is shown in Figs. 31–34. Degradation rates relative to initial outputs for the short-circuit current, radiation-resistant short-circuit current, and open-circuit voltage cells were approximately 14, 5, and 3%, respectively. Solar array output telemetry data did not indicate degradation, and the ability to determine degradation from the voltage and current outputs was restricted by: (1) the early limiting of solar array output by the zener diodes, and (2) the later operation of the array, far down on its current–voltage curve, close to the open-circuit voltage.

The degradation that was observed in the $I_{sc}-V_{oc}$ transducers appeared to be smooth and continuous. The rate of degradation does not indicate that this rate is a function of spacecraft heliocentric distance, and its smoothness is not indicative of radiation damage by solar flares. Furthermore, spacecraft instrumentation did not detect significant high-energy proton fluxes. The most likely environmental causes of this change are heat and ultraviolet energy. Results of studies conducted at JPL to observe elevated-temperature effects on solar cells do not indicate that a degradation of this magnitude should be expected. The zener shunt regulation of the array appeared to perform as predicted. Review of the data presented in Fig. 32 and Table 5 indicates that the solar array power output was predicted to go off zener diode regulation on approximately day 90. The analytical techniques used in this evaluation are supported by: (1) the intersection of the spar temperature telemetry curve with the predicted temperature curve for a spar with no power being dissipated in the zeners, and (2) the relatively significant change of array voltage after day 90.

Table 5. Summary of predicted and measured solar array performance

Time from launch, days	Solar intensity, mW/cm²	Temperature, °C			Voltage, V		Current, A	
		Panel sensor	$I_{sc}-V_{oc}$, $I_{sc}R^a$ transducers	Spar sensor	Predicted zener diode	Measured solar array (PS&L[b] voltage +0.7 V)	Measured solar array	Predicted solar panel assuming zener diode load
1	135.7	46.6	40.5	33.9	48.15	47.86	3.62	8.86
10	138.1	49.6	42.8	35.1	48.15	47.86	3.63	8.86
20	142.0	51.9	45.0	36.2	48.15	47.86	3.75	8.98
30	146.9	55.4	48.5	38.6	48.15	47.86	3.76	9.21
40	153.5	59.0	52.2	41.0	48.15	48.11	3.75	8.99
50	162.6	64.0	57.3	43.4	48.15	48.11	3.79	9.06
60	172.8	70.2	63.6	47.0	48.12	48.11	3.79	8.66
70	185.4	77.4	70.0	48.3	48.01	47.86	3.89	8.66
80	199.7	84.5	75.6	49.5	48.05	47.86	3.83	8.15
90	216.0	92.4	86.0	50.7	47.9	47.38	3.83	6.57
100	232.9	100.9	93.0	52.0	—	46.67	3.87	3.87
110	248.7	106.5	100.0	55.6	—	45.46	3.95	3.95
120	262.2	112.4	105.0	59.5	—	44.53	4.07	4.07
125	267.2	114.0	107.2	60.8	—	44.12	4.12	4.12
127	268.7	115.6	108.1	62.0	—	43.88	4.11	4.31
130	272.4	116.1	108.8	62.0	—	43.59	4.50	4.50
140	278.3	121.5	114.5	65.9	—	43.12	4.19	4.19
145	283.4	124.8	117.5	67.1	—	42.65	4.19	4.19
150	301.5	127.5	120.8	69.8	—	41.01	4.38	4.38

[a]Radiation-resistant short-circuit current cell.

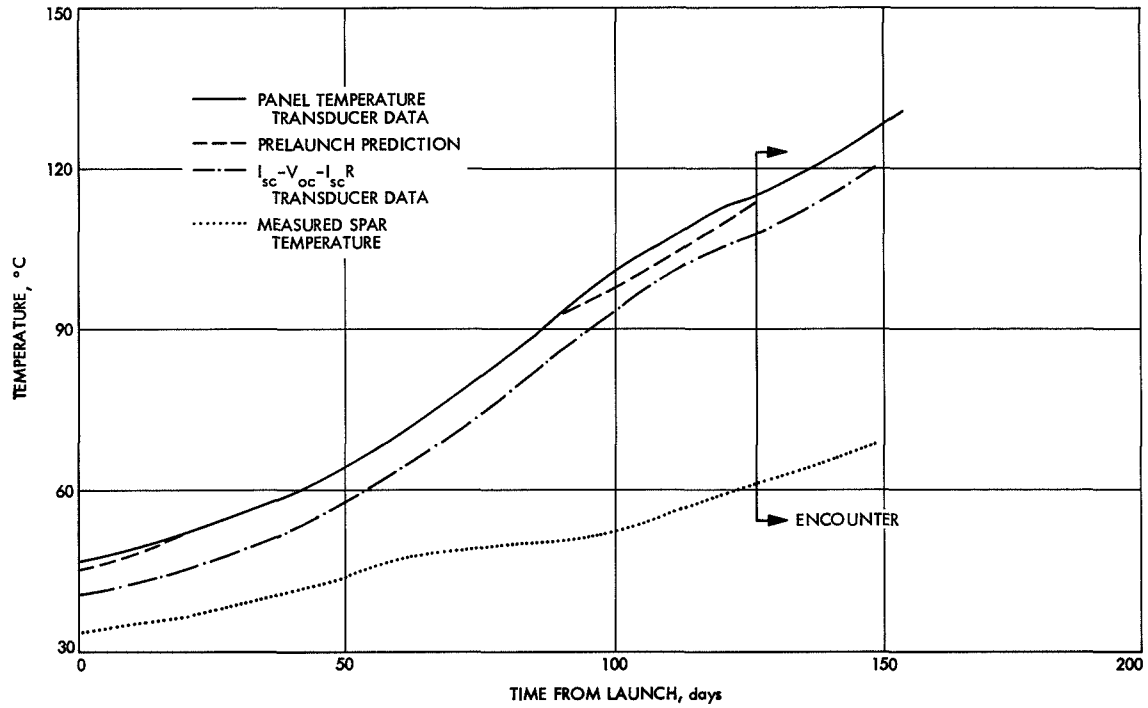[b]Power switch and logic.

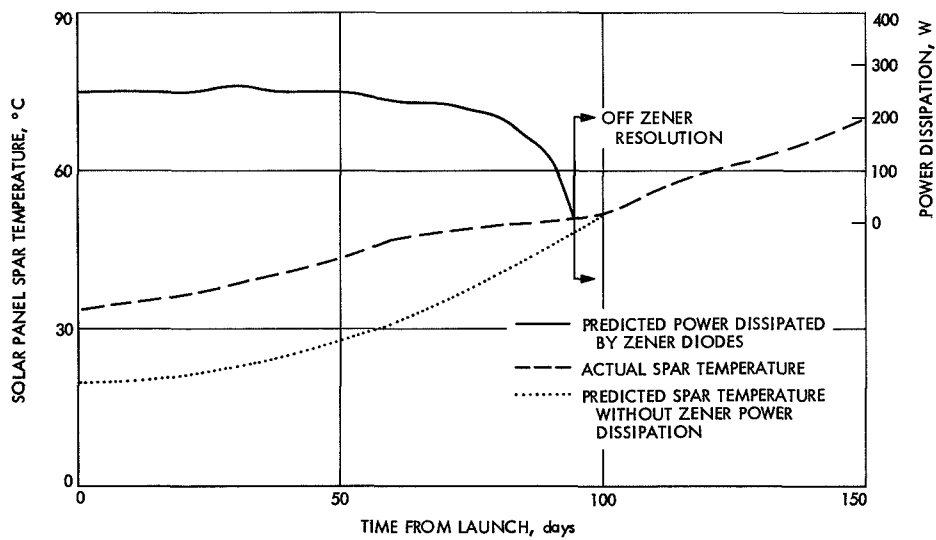**Fig. 31. Predicted vs actual temperature data, *Mariner* Venus 67 solar panels**

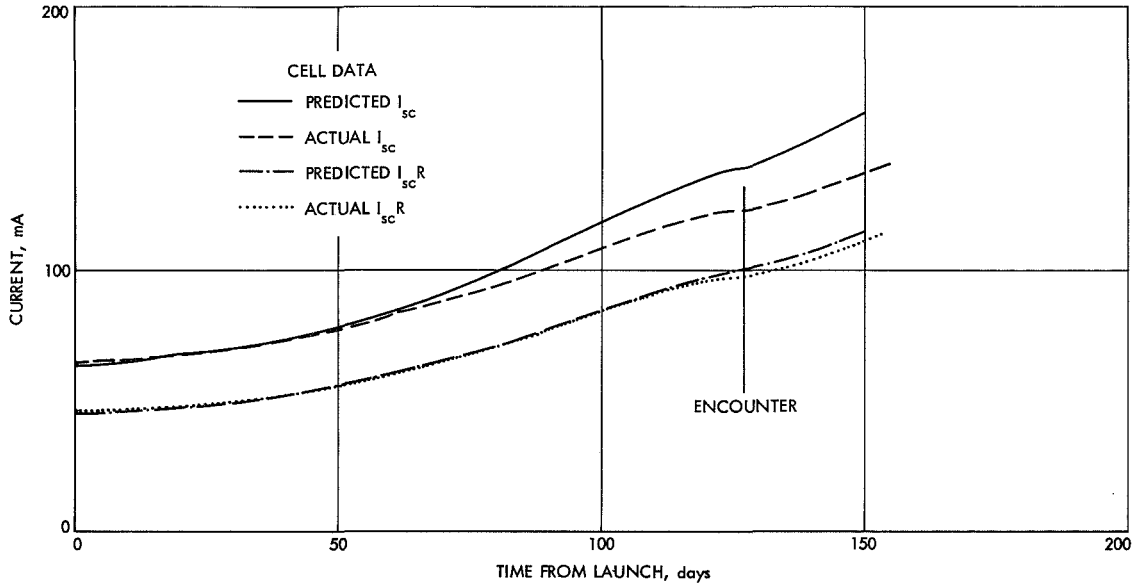**Fig. 32. Predicted vs actual spar temperature data**

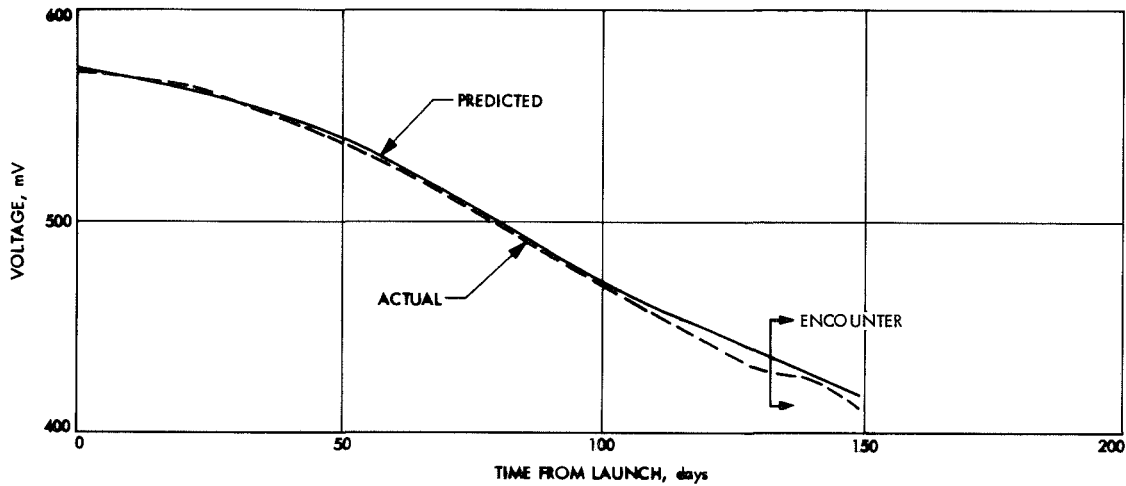**Fig. 33. Predicted vs actual current, short-circuit current and radiation-resistant short-circuit current cells**

Fig. 34. Predicted vs actual voltage, open-circuit voltage cell

VII. Conclusions and Additional Remarks

Generally, the solar array design proved adequate for this mission. This experience, together with results of supplementary tests at JPL, indicates that present materials and technology can result in significantly better design than that used on the *Mariner* Venus 67 solar array. Future designs of *Mariner* Venus 67-type solar panels should consider, in place of the material list shown in this report, 1-Ω-cm n-on-p cells with sintered contacts. Kovar was a satisfactory bus bar material; however, care should be exercised in providing good stress relief. For example, a 3-mil tin-plated ribbon would be a better top cell contact bus bar than the 20-mil gold p bus wire that was used in this design.

28

JPL TECHNICAL REPORT 32-1321
NASA — JPL — Coml., L.A., Calif.